REVISTA MATÉRIA V.31
ISSN 1517-7076 articles e20250329, 2026

Concrete reinforced with polymeric fibers: an approach by non-destructive techniques of ultrasonic pulse velocity and electrical resistivity

Rayane Campos Lopes[1], Cibele de Moura Guimarães[1], Patrícia Guedes Gambale[1], Andrielli Morais de Oliveira[1]

[1]Universidade Federal de Goiás, Escola de Engenharia Civil e Ambiental, Laboratório de Inovação Tecnológica em Construção Civil. Goiânia, GO, Brasil.

e-mail: rayaneclopes@discente.ufg.br, cibeleguimaraes@discente.ufg.br, patricia.gambale@gmail.com, andriellimorais@ufg.br

ABSTRACT

The primary objective of incorporating fibers into concrete is to enhance its load-bearing capacity subsequent to cracking, thereby demonstrating its augmented toughness. Additionally, the incorporation of fibers into concrete has been demonstrated to enhance safety, utility, service life, performance, and durability of concrete structures, particularly in terms of crack control. Non-destructive testing are important tools for inspection and monitoring the integrity and service life of reinforced concrete structures. This research evaluated the mechanical performance, electrical resistivity (surface and bulk) and ultrasonic pulse velocity of concrete reinforced with polymeric fibers. Three different volumes (V_f) of copolymer-based fibers (0.5%, 1.0% and 1.5%) were considered. The type of concrete with polyethylene/polypropylene-based fibers was also considered with a V_f of 1.0%. Tests were conducted to determine the material's compressive strength, modulus of elasticity, and flexural tensile strength, as well as surface electrical resistivity, bulk resistivity, and ultrasonic pulse velocity. A detailed discussion of the results was conducted, with particular reference to statistical analyses, micro-mechanisms and correlated data. Consequently, an increase in V_f had a negative effect on the compressive strength and modulus of elasticity. As expected, there was a significant increase in the residual flexural tensile strength. An increase in V_f tends to reduce resistivity, particularly surface electrical resistivity, while the ultrasonic pulse velocity remains essentially unchanged. The optimum V_f of copolymer-based concrete of this study was determined to be 1%, and the performance of the three types of fibers studied (copolymer-based and polyethylene/polypropylene-based) was found to be "equivalent". A comprehensive evaluation of the properties revealed that FRC (Fiber-Reinforced Concrete) exhibited distinct advantages, particularly with regard to its residual flexural tensile - strengths.

Keywords: Mechanical Performance; Polymeric Fiber; Non-destructive Testing; Ultrasonic Pulse Velocity; Electrical Resistivity.

1. INTRODUCTION

In the civil construction industry, the demand for durable concrete structures is driven by the necessity to minimize maintenance and repair costs, as well as the frequency of interventions of maintenance and repairs throughout the structure's service life and lifecycle [1–3]. In this regard, fibers have proven to effectively enhance the mechanical properties of concrete, including its tensile and flexural strength, ductility, strain capacity, post-peak behavior, and toughness [4–6]. In addition, the use of the fiber-reinforced concrete (FRC) has been shown to durability and performance under adverse field conditions, such as low vacuum drying environments (100 Pa) [7], chemical exposure [8], chloride attack, high temperatures [9], sulfate attack, dry-wet cycles [10], and combined effects of temperature and moisture [11].

The characteristics of FRC are known to be contingent on several a number of factors, including the mixing procedures, casting, the cementitious matrix, the matrix-fiber interface, and the properties of the fibers. These properties include their material, geometry, surface, stiffness, tensile strength, fiber volume fraction, shape, orientation, and distribution in the matrix [4, 12–16]. Fibers can also be classified, according to their origin, into natural fibers, such as cellulosic fibers [17, 18], mineral-based (basalt) [13–17], and synthetic fibers,

Corresponding Author: Andrielli Morais de Oliveira Received on 16/04/2025 Accepted on 27/10/2025

DOI: https://doi.org/10.1590/1517-7076-RMAT-2025-0329

such as steel fibers [20, 21], polymer fibers [22–24], and glass fibers [25, 26]. Moreover, synthetic fibers, as polyethylene (PE) and polypropylene (PP) are generally more resistant to water, heat, and chemical degradation than natural fibers, including coconut and sisal fibers [27]. Furthermore, polymeric fibers are produced on a large scale and they have versatile applications, including textiles, the automotive industry, laboratory equipment, civil construction, and reusable packaging [28].

According to the standard EN 14889-2 [29] polymer fibers are defined as straight or deformed pieces of extruded, oriented, and cut material suitable for homogeneous mixing into concrete or mortar. Consequently, this standard establishes a classifications system that includes: micro fibers and macro fibers.

The classification system in question has been developed to facilitate the differentiation of these fibers based on their diameter and function in concrete applications. Consequently, the macro fibers, with a mean length ranging from 30 mm to 50 millimeters, are designated as structural fibers due to their capacity to transfer the loads exerted on the structure and to substitute for conventional steel bar reinforcement. In contrast, micro-fibers, measuring less than 30 mm, have the function to mitigate the formation of small cracks in concrete, such as those induced by plastic shrinkage. This, in turn, enhances post-cracking behavior [17].

Moreover, polymeric fibers are recyclable [28] and can offer advantages such as lower fiber consumption per cubic meter of concrete and a superior final surface finish when compared to metallic fibers. They can also reduce operational expenses relative to welded wire mesh, with the added benefit of preventing corrosion. In thin concrete structures, polymeric fibers can further decrease construction time and costs compared to wire mesh or steel fibers [30–33] as they eliminate the need for storage, handling, cutting, and the associated material losses. Additionally, they provide non-magnetic and non-conductive reinforcement. The selected fibers are capable of improving crack control, plastic shrinkage performance, corrosion resistance, as well as resistance to impact, fatigue, shear, and abrasion. Owing to their geometry, these fibers can provide adequate anchorage within the matrix, functioning effectively as short, staple fibers that are randomly dispersed and three-dimensionally oriented in the concrete [12, 34].

Besides that, polymeric FRC enables the construction of thinner pavements with lower embodied energy in the final product [35], decorative pavements, fountains, sculptures, artificial rocks, and skate parks [31]. Its use also extends to pavements industrial and commercial floors, airport runways, and parking lots, tunnels, slab-on-grade foundations, concrete pipes, blast-resistant structures, shotcrete applications, slender structures elements, parking lots, walls and panels, basements, road pavements, overlays, thin precast elements, and garage basements [36–38]. In many of these applications, polymeric fibers offer the potential for cost reduction by replacing high-modulus steel fibers [39].

In a similar manner, studies have shown that FRC containing PE fibers (0.75% and 1.50%) exhibit strain-hardening behavior, whereas FRC reinforced with PP demonstrates brittle fracture behavior. However, under compressive loading, both PE and PP-reinforced FRCs exhibit ductile failure. Nevertheless, PE-reinforced FRC established a higher ultimate load capacity and superior post-peak ductility. The performance has been attributed to the low-vacuum condition, which enhances fiber-matrix interfacial bonding and increases energy dissipation during both fiber debonding and pullout. So, this mechanism promotes strain-hardening in PE FRC [7]. Conversely, Palanisamy and Ramasamy [40] investigated the mechanical properties of polypropylene-reinforced FRCs. The concrete mix containing 2% polypropylene fibers demonstrated only a marginal enhancement in average compressive strength [40].

However, Islam and Waseem [41] investigated the mechanical and fracture properties of concretes reinforced with polypropylene fibers. The incorporation of polypropylene fiber resulted in a slight reduction in compressive strength, while producing the most substantial increase in the concrete's split tensile strength. In another study, Castoldi *et al.* [42] reported that polypropylene fiber reinforcement reduced crack propagation and widening, while enhancing the flexural toughness, fatigue resistance, and impact resistance of the concrete.

Other research has observed that the addition of polyvinyl alcohol (PVA) fibers significantly enhances the flexural strength of cementitious composites through effective fiber bridging, although their contribution to improvements in compressive strength remains minor [43]. In fact, fiber-reinforced concrete can exhibit increases, maintenance, or even reduction in compressive strength, depending on variables related to the fiber phase, the matrix, and the matrix-fiber interface, as well as the mixing, molding, and compaction procedures of the cementitious mixture [4, 13–15]. Nevertheless, in general, some ductility and post-peak load-bearing capacity are retained compared to concrete without fibers [44].

Non-destructive testing (NDT), including ultrasonic pulse velocity (UPV) and resistivity measurements, comprises methods for evaluating concrete structures without causing damage. NDT can be considered a complementary tool for in-situ inspections and for monitoring the integrity and service life of structures. In addition,

these techniques have gained widespread recognition due to their extensive use in both -professional practice and scientific research. They are cost-effective, rapid, and allow for in-situ and laboratory evaluation [40].

Regarding UPV, this technique has great potential for assessing concrete homogeneity, as it can identify flaws, localized defects, and non-conformities in batches or regions of structural or non-structural concrete, with or without fibers [45]. Numerous studies have established a strong exponential correlation between UPV values and the compressive strength of cementitious composites.

This highlights the strong potential of these techniques for estimating concrete strength analyses in this field must conducted with caution, as numerous factors can cause deviations between estimated and actual strength values [46, 47]. Indeed, higher UPV values indicate uniformity and relatively good quality of concrete, including FRC, whereas lower UPV may signify the presence of cracks or voids and defects. Cánovas [48] relates concrete quality to the UPV values. According to this classification, values below 2000 m/s are associated with concrete of regular and poor quality, values above 3000 m/s indicate good quality, and values exceeding 3500 m/s correspond to concrete of very good to excellent quality [48].

Acebes *et al.* [49] investigated the effect of steel fibers on the ultrasonic velocity of FRC. By combining micromechanics analysis with ultrasonic velocity concept, and considering capillary porosity, air voids, and steel fiber inclusions. They found that ultrasonic velocity decreased as the volume fraction of steel fiber increased. Alharthai *et al.* [50] used UPV technique to evaluate concrete containing varying amounts of recycled aggregates and polypropylene fibers (1%, 2%, and 3%) with a length of 12 mm, along with fly ash and silica fume. In all the concretes made with only natural aggregates, the addition of fibers increased the wave propagation velocity, with a 27% increase observed after 28 days in the concrete containing 3% fibers compared to the concrete without fiber. The UPV of fiber-reinforced concrete increased with the fiber volume fraction (V_f) compared to reference concrete. Improvement can likely be attributed to the presence of mineral additions. UPV values of 2650 m/s were found in concrete without fibers, while 4900 m/s were recorded in concrete with fibers.

Castillo and Hedjazi [51] investigated the correlation between dynamic modulus and compressive strength of FRC containing nylon, polypropylene, stainless steel, and glass fibers, and UPV at early ages. The addition of nylon and polypropylene fibers (19 mm length) reduced the UPV related to plain, likely due to lower densities and reduced workability, which resulted in more voids. In another study, Yazici *et al.* [52] estimated the splitting tensile, compressive, and flexural strengths of steel fiber-reinforced concrete (SFRC), considering the fiber volume fraction and the aspect ratio. They established several empirical relationships between fiber strength reinforcement and UPV.

Electrical resistivity (Re) is a physical property that serves as an indicator of concrete durability and is a valuable parameter for the inspection, evaluation, and diagnosis of reinforced concrete structures, with or without pathological issues. Being completely non-destructive, the Re technique can be used associate with other methods and employed for specification and quality control of concrete both in the field and in the laboratory [53, 54].

Furthermore, researches have shown that electrical resistivity is a highly versatile technique. Its results can indicate different variations in concrete compositions, porosity, and permeability, differences in moisture or saturation levels, aggregate segregation, self-healing behavior, hydration of alkali-activated materials, and the presence even at early stages of aggressive agents, particularly chlorides and sulfate [46, 55–66]. Re enables the application of surface response and machine learning techniques to predict concrete properties based in resistivity measurements [67]. However, this technique is also influenced by factors such as sample size and geometry, electrode spacing , and the concrete internal moisture condition of the concrete [46, 68–70].

The literature correlates surface electrical resistivity (Re) values with the probability of corrosion of steel reinforcement in concrete. Higher resistivity values generally indicate of low internal moisture or low probability of corrosion of steel reinforcement in concrete (above 20 kΩ.cm). Resistivity values between 10 and 20 kΩ. cm are associated with low probability of corrosion, values between 5 and 10 kΩ.cm indicate high probability, and values below 5 kΩ.cm correspond to a very high probability of corrosion [71].

Also, logarithmical approach has been established between electrical resistivity and compressive strength for concrete without fibers, with an R-Squared (R^2) value exceeding 0.98. Both parameters are directly proportional, meaning that higher compressive strength corresponds to higher electrical resistivity [72]. This behavior has also been noted in other studies [73, 74] and it is attributed to the clear influence of porosity on both properties. Araujo and Meira [75] found correlation curves between compressive strength and surface electrical resistivity, as well as between splitting tensile strength and surface electrical resistivity for Brazilian concretes without fibers. These relationship are expressed $fc = 14.18 \cdot \ln(\rho) + 18.43$ and $ft = 0.69 \cdot \ln(\rho) + 2.15$ for compressive strength and splitting tensile strength, respectively.

The presence of fibers, as well as their type and content, can alter the electrical resistivity values of cementitious materials. [76] studied the electrical resistivity of different types of mortars containing carbon and PVA (polyvinyl alcohol) fibers. Mortars reinforced solely with PVA fibers showed significantly higher resistivity than those with only carbon fibers. Moreover, increasing the PVA fiber content led to a decrease in resistivity. [77] analyzed the electrical resistivity of concrete containing conductive fibers (steel) and non-conductive fibers (macro-polypropylene, micro-polypropylene, and micro-nylon), with and without silica fume. The results showed a slight reduction in bulk resistivity with the addition of non-conductive fibers in plain concrete, along with minimal variation in surface resistivity.

The objective of this work is to evaluate the mechanical performance (compressive strength, modulus of elasticity, and flexural tensile strength) at 28 days of polymeric fiber-reinforced concretes, considering different fiber types and contents, while also analyzing surface and bulk resistivity and ultrasonic pulse velocity (UPV).

1.1. Research significance

The paper makes significant contributions to the scientific and technological fields. It presents experiments with various volumes of polymeric fibers and evaluates their impact on the mechanical performance of concrete, including compressive strength, modulus of elasticity, and tensile strength. In addition, non-destructive techniques and durability indicators were employed to assess the Brazilian fiber-reinforced concretes. These indicators included surface and bulk electrical resistivity and ultrasonic pulse velocity.

The use of UPV has been shown to facilitate the estimation or prediction of the behavior of concretes produced in batching plants with various types and volumes of fibers.The data obtained were subjected to statistical analysis and correlation assessment. An effort was made to explain the results and their trends in terms of macro-, meso-, and micro-scale mechanisms. Consequently, the findings of this study provide valuable insights for engineers and practitioners involved in the design and application of fiber-reinforced concretes.

In Brazil, several standards for fiber-reinforced concrete have been published in recent years (2021). The construction market and consumers are currently adapting to these new regulations. These standards cover the design of fiber-reinforced concrete structures [78], the determination of cracking and residual tensile strengths using the double-punching method [79], and the quality control of fiber-reinforced concrete through the assessment of flexural tensile strengths (proportionality limit and residual strengths) [80]. Standard [78] exhibits technical equivalence with the European standard EN 14651 [81], which also establishes criteria for evaluating the residual flexural tensile strength of fiber-reinforced concrete. Additionally, it establishes standardized procedures for obtaining parameters such as fR1 and fR3 in performance-based design [78], thereby facilitating international comparison and the practical application of the results [81]. The performance of fiber-reinforced concretes produced with Brazilian materials requires further investigation, particularly concerning durability.

In addition, the present paper aligns with the United Nations Sustainable Development Goals specifically Goals 5, 8, 9, 11, 12, 13, and 17. The paper proposes the implementation of public-private partnerships to strengthen regional and local civil construction markets and advocates for greater female authorship in academic publications. The study emphasizes the importance of durability, longevity, and performance of reinforced concrete structures, aiming to reduce the consumption of natural raw materials and minimize the need for premature maintenance.

2. MATERIALS AND METHODS

In this research, Brazilian concrete mixtures were evaluated to analyze the type and volume of fiber (V_f) and its correlation with UPV and resistivity data in mechanical behavior. Thus, several types of concretes were produced: one type reference (without fibers) and three types with copolymer fibers at different volumes (0.5%, 1.0% and 1.5%). Two types had a fixed fiber dosage of 1% with a mix of polyethylene and polypropylene fibers from different suppliers.

Besides that, the concrete mix design was based on plot chart and preliminary tests conducted at the concrete plant for urban concrete pavements and concrete floors. Thus, the compressive strength of fiber-reinforced concrete must be within the range of 35 MPa to 45 MPa, and its minimum tensile strength in bending must be a minimum of 3.8 MPa (roads with commercial vehicle traffic). Additionally, the minimum cement consumption must be 300 kg/m^3, and harder aggregates must be used, as described in [82, 83, 84].

2.1. Materials

The concrete constituents employed in this study included Portland cement as a primary binder, fine and coarse aggregates, water and a chemical admixture. Thus, the Brazilian Portland cement type CP V (composed of

0-10% in mass of limestone filler and 90-100% of clinker - with a small amount of calcium sulfate) was used. This cement type has a minimum compressive strength requirement of 14 MPa at the age of 1 day [85], which is similar to the American cement Type III [86]. Also, this cement is in accordance with Brazilian standards specifications. In addition to, two types of sand (see Figure 1a) and coarse aggregates (two gneiss crushed rocks) (see Figure 1b) [87], were used [88]. According to ACI 544 [15], the utilization of coarse aggregates with dimensions exceeding 19 mm is not recommended for fiber concretes because of the workability and consistency requirements. The specifications of other materials and the characterization tests conducted are provided in Tables 1 and 2.

The water-reducing chemical admixture was used to enhance workability and reduce water content. It possessed a specific gravity of 1.11 g/cm^3, 24.55% solid content and pH of 5.21 [89] similar to [90]. Tap water, defined as potable water from the public distribution network was utilized [91, 92]. These materials were chosen based on local availability. Three types of polymeric fibers of low modulus [93, 94] were added to the concretes studied (see Figure 2). The technical characteristics of the fibers are presented in Table 3. These types of fibers are used in Brazil in commercial concrete plants for various applications, including for industrial and commercial flooring. The employment of these fiber types offers the advantages of reduced fiber consumption per cubic meter of concrete and an enhanced final concrete finish in comparation to metal fibers [77, 94, 95]. Furthermore, these polymeric fibers can be used in a variety of other applications in concrete, including parking lots, walls and panels, basements, slabs-on-grade, concrete pavement in slab format and molded in situ, road pavements and overlays, steel slabs, thin precast elements and garage basements [30, 32, 33, 36–38].

a) b)

Figure 1: Material used: (a) fine and (b) coarse aggregates, respectively.

Table 1: Chemical and physical properties of the Portland cement used.

MATERIAL	CHEMICAL COMPOSITION (%)		INSOLUBLE RESIDUE (%)***	LOSS ON IGNITION (%)****	SPECIFIC GRAVITY (g/cm^3)	SPECIFIC SURFACE AREA (m^2/kg)	COMPRESSIVE STRENGTH (MPa)*****		
	MGO**	SO_3*					1 DAY	7 DAYS	28 DAYS
Brazilian cement CP V ARI [89]	4.83	4.12	3.32	2.59	3.08	501.6	26.7	39.8	47.3

According to Brazilian standard [89] for this type of cement these properties must be less than or equal to the *sulfur trioxide 6.5; **magnesium oxide 4.5; ***Insoluble Residue 6.5; ****loss of ignition 3.5 and ****compressive strength requirement minimum at the age of 1 day 14 MPa and 34 MPa at age of 7 days [89].

Table 2: Properties of the fine and coarse aggregates.

PROPERTIES	UNIT	NATURAL SAND	CRUSHED SAND	GRAVEL 1	GRAVEL 0
Specific gravity	g/cm^3	2.62	2.78	2.89	2.82
Maximum nominal size	mm	0.60	4.80	19.0	12.5
Fineness modulus	–	1.17	2.70	5.90	5.90
Powder content amount	%	0.48	4.70	0.21	1.27

Figure 2: The fibers A (copolymers-based), B and C (Polyethylene and polypropylene mix-based) used.

Table 3: Technical characteristics of the fibers used.

CHARACTERISTICS	A	B	C
Base Polymer [94]	Copolymers	Polyethylene and polypropylene mix	Polyethylene and polypropylene mix
Specific gravity (g/cm^3)	0.91	0.91 – 0.92	0.92
Length (mm)	51	58	51
Aspect ratio L/D	79	No informed	74
Tensile strength (MPa)	620 – 685	640	600 – 650
Elastic modulus (GPa)	5	10	9.5
Quantity recommended by the manufacturers (kg/m^3)	1.8 – 3.0	2.5 – 5.0	1.8 – 12.0
Commercial name	TUF-STRAND Maxten	BarChip MQ58	TUF-STRAND SF
Appearance	Monofilament	Short and single	Monofilament
Type of grouping [949]	Grouped in bundles		

2.2. Concretes

Table 4 presents the concrete mixtures proportions.

The fiber A was incorporated into the concrete in percentages of fiber volume (V_f) of the 0.5%, 1.0%, and 1.5% by mass relative to the cement content. In order to conduct a comparative study, fibers B and C were added with a V_f of 1.0% content. These V_f are justified because they are the most commonly used in projects requiring fiber-reinforcing concrete in the region of this research. This is based on the literature [77, 95–97].

Cement consumption was kept constant level. The slump test was controlled to ensure adequate workability. The measurement of 135 ± 10 mm (S-100 class between 100 mm < slump < 160 mm) was recorded for concrete structural elements with conventional casting [98–100] similar to [101].

It is known that the incorporation of fibers into concretes changes the rheology, workability and consistency. This phenomenon was observed to occur with minor variations in diameter, with an average measurement of 135 ± 10 mm, as depicted in Table 4. Thus, an unfavorable combination of cement matrix properties, fiber-matrix interface properties, fiber (V_f, type, material, shape, and length), and mixer power and mixer speed can result in inadequate fiber dispersion and homogenization in the mix, agglomerations, lump formation, and significantly reduced workability, casting capacity, and compaction, even with the use of chemical admixtures and mineral addition [4, 13, 14]. So, as expected, the incorporation of fiber-reinforcing reduced the workability of the all concretes studied (Table 4), with the exception of C1.5A, which exhibited an augmented water content.

At the same time, a greater volume of fibers can result in a change of speed of propagation of ultrasonic waves, due to formation of voids and or clumping. Furthermore, although large volumes of fiber are desirable from the point of view of improving mechanical behavior, practical application limitations may occur (greater

Table 4: Proportions of concrete mixtures and slump in the fresh state.

CONCRETE TYPES	CONSTITUENT (kg/m³)									WATER/ CEMENT RATIO	SLUMP (MM)	CONCRETE COST ($/m³)*
	CEMENT	FIBER	TYPE OF FIBER	CRUSHED SAND	NATURAL SAND	GRAVEL 0	GRAVEL 1	WATER	ADMIXTURE			
REF	390	–	–	400	400	216	862	205	2.73	0.526	145	117.72
C0.5A	390	1.95	100% pure copolymer	400	400	216	862	210	2.73	0.538	130	130.26
C1.0A	390	3.90		400	400	216	862	217	2.73	0.556	135	135.42
C1.5A	390	5.85		400	400	216	862	220	2.73	0.564	145	153.14
C1.0B	390	3.90	Polyethylene/ Polypropylene mix	400	400	216	862	217	2.73	0.556	135	144.89
C1.0C	390	3.90	Polyethylene/ Polypropylene mix	400	400	216	862	217	2.73	0.556	140	148.15

*It was considered that $1.00 was equivalent to R$ 5.42.

than 2%), from the point of view of mixing, workability, molding and compaction of fiber-reinforcing concretes [4, 13, 14, 36].

Since the fibers can absorb some water during mixing, more water was added to achieve the applicable slump. This altered the water-to-binder ratio (w/b) between of the studied mixes. Table 4 indicates as that the fiber volume increased from 0.5% to 1.5% (copolymer-based fiber), a small amount of additional of water was required, resulting in a s slight increase in workability, from 130 mm to 145 mm, as measured by the slump test [99–101]. Otherwise, when comparing concretes with same V_f (1.0%) and the same amount of water and chemical admixture, only the concrete with C fiber had a higher workability value (140 mm). This could be result of the different types of fibers, their geometry, surfaces, and fiber-matrix interfaces.

The concretes were produced in a stationary unit using a mechanical mixer. It was considered the fiber types, mixing time, mixer energy of mixer and workability of concretes to prevent clumping and segregation on the concrete. The fibers were introduced into the concrete mixture after the cement, aggregates, water, and chemical admixture to prevent clumping and ensure uniform dispersion (Figure 3). After adding all the components, the mixture was kept under constant agitation at high speed for 5 minutes. This controlled process ensured the homogeneity of the mixture and the dispersion of the fibers, thereby improving the concrete's performance.

Next, the specimens were molded using mechanical vibration (a needle-type immersion vibrator). Cylindrical and rectangular concrete specimens were molded for testing in a hardened state [102]. Samples with dimensions of 10 × 20 cm (diameter and height) were molded in one layer for while the rectangular specimens (15 × 15 × 60 cm) were molded in three layers. After molding, plastic films were applied to the specimens' surface and before demolding. At the age of three days, the specimens were demolded and placed in a controlled chamber with controlled humidity and temperature (an average 95% humidity and 25°C) until the of age of testing.

2.3. Mechanical and Non-destructive Testing Methods

Figure 4 shows the setup for the compressive strength, modulus of elasticity; surface electrical resistivity (with 50 mm and 38 mm probe spacing), bulk resistivity and ultrasonic pulse velocity tests. At the age of 28 days, the specimens were tested. Three sample replicas were used. The concrete specimens were tested using a mechanical test, i.e., compressive strength [103], similar to [104, 105], modulus of elasticity [106,107], and flexural tensile strength [80, 82].

The specimens for compressive strength, modulus of elasticity, surface electrical resistivity, bulk resistivity and ultrasonic pulse velocity tests were cylindrical with dimensions of 100 mm in diameter and 200 mm in height, as mentioned before. Also, for the flexural tensile strength test, the specimens were prisms with dimensions of 150 × 150 × 600 mm.

Compressive strength tests were development using neoprene discs confined in metal supports (Figure 4a). The tests were performed using an EMIC PC200 machine coupled with an EMIC DL 30000 electromechanical machine, with a 2000 kN load cell, at a loading speed of 0.45 MPa/s.

a) b)

Figure 3: The addition of fiber into the concrete (left) and concrete in the fresh state (right).

Figure 4: Mechanical test experimental setup for cylindrical specimens: (a) compressive strength test and (b) static modulus of elasticity test under compression.

Static compression modulus of elasticity tests, also known as the initial tangent deformation modulus tests, were performed in accordance with, obtained from the angular coefficient of the line tangent to the stress-strain curve between 0.5 MPa and 30% of the compressive strength (fc) of the evaluated mixture. The tests were performed on cylindrical concrete specimens with nominal dimensions of 10 cm × 20 cm using an EMIC DL30000 electromechanical press with a 300 kN load cell, as well as a compressometer with independent bases and dial gauges with a resolution of 0.001 mm.

The flexural tensile strength test was the most complex, performed according to NBR 16940 [80] and used the same press as the modulus of elasticity test. This is a recent Brazilian standard, specific to fiber-reinforced concrete, based on international standards, such as the European standard EN 14651 [81] and the American ASTM C1609 standard [108].

The test consists of prismatic test specimens in a three-point bending setup with a simply supported beam (500 mm span) and a load applied by a roller in the middle of the span, above the notch. The test was performed in a closed-loop speed control system with a constant crack mouth opening displacement (CMOD) rate. The samples tested were prismatic concrete prisms with a cross-section of 15 cm × 15 cm and a total length of 60 cm. To induce cracking in a specific location, a 4 mm notch was made in the middle of one of the lateral faces of the molding surface, which is smaller than the 5 mm specified by the standard.

To measure the crack opening, a transducer was connected to two metal plates, glued to the faces of the notch. In the test, the load is applied variably to ensure the notch opening remains constant at a rate of 0.05 mm/min until CMOD = 0.1 mm, after which the rate is 0.2 mm/min. The test must continue until a minimum opening of 4 mm is reached.

The main results of the test were: the limit of proportionality (LOP) and the residual flexural tensile strength (f_{Ri}), given respectively, by Equation 1 and Equation 2.

$$f_L = \frac{3F_L l}{2 b h_{sp}^2} \tag{1}$$

Where: f_L = limit of proportionality – LOP (N/mm^2); F_L = load corresponding to the LOP, being the maximum load in the range of 0 to 0.05 mm (N); l = span length between supports (mm); b = width of the specimen (mm); and h_{sp} = distance between the tip of the notch and the top of the specimen (mm).

$$f_{Ri} = \frac{3F_i \iota}{2 b h_{sp}^2} \tag{2}$$

Where: f_{Ri} = residual flexural tensile strength, corresponding to CMODi – i (1, 2, 3, 4), corresponding to 0.5 mm, 1.5 mm, 2.5 mm, and 3.5 mm (N/mm²); and F_i = load corresponding to CMODi – 0.5 mm, 1.5 mm, 2.5 mm, and 3.5 mm (N).

Based on the load vs. CMOD curve, the fracture energy was calculated using Equation 3, according to RILEM TC FMC-50 recommendations [109].

$$G_f = \frac{w_0 + m g \delta}{b h_{sp}} \tag{3}$$

Where: G_f = fracture energy (N/mm); Wo = is the area under load-deflection (N.mm); m = mass (weight) of the sample (concrete beam) between the supporting rollers (kg); g = gravitational acceleration (9.81 m/s²); δ = deformation at the final failure of the beam (maximum defection) (mm), b × h_{sp} = corresponds to the crack path area (the area over the notch).

Non-destructive tests were conducted on the studied concretes. Thus, surface resistivity tests, bulk resistivity [110–112], and ultrasonic pulse velocity [113, 114] were performed (Figure 5). All the resistivity tests were determined by constant-frequency electrical resistivity. The device used digitally generated 40 Hz alternating current. Superficial resistivity was based on Wenner's principle. The Resipod (Proceq) equipment was used, with a nominal probe spacings of 38 mm and 50 mm and with 4 electrodes between the probes (Figura 5ab). Measurements were taken on 3 cylindrical test specimens for each mix. Each sample, 3 equidistant measurements were made on the lateral surface, for a total of nine measurements per mix for each device. The result was the average of these 9 values. The same number of measurements were taken for all non-destructive tests.

For the volumetric method, a system consisting of two coupled circular electrodes measuring 102 × 102 mm was used for axial reading (Figure 5c). The system offers the option of using either 102 mm × 102 mm circular electrodes for concrete samples or 42 mm × 42 mm square electrodes for mortars and pastes. In both operating modes, the device uses a digitally generated 40 Hz alternating current. Measurements were taken on 3 cylindrical test specimens for each mix. Bulk electrical resistivity was measured using the same Resipod device with metal plates (Figure 5c).

Surface electrical resistivity was measured using the Wenner method with two different devices, both with 4 electrodes but with different spacing. The "Resi" device from Proceq manufacture has an electrode spacing of 50 mm, and the "Resipod" device, also from Proceq, has a spacing of 38 mm. Each device uses digitally generated 40 Hz alternating current in all operating modes.

Surface resistivity (ρ_s) measured by the Wenner method is given by:

$$\rho_s = \frac{2\pi a V}{I} \tag{4}$$

where a is the probe spacing (a = 37.5 mm), I is the applied current, and V is the potential difference measured by the Resipod.

a) b) c) d)

Figure 5: The non-destructive tests used: (a) and (b) surface resistivity tests, (c) bulk resistivity test and (d) ultrasonic pulse velocity test.

For cylindrical specimens, a geometric correction factor k must be applied. This factor is defined by equation 5 [115].

$$k = \frac{2\pi}{1{,}09 - \frac{0{,}527}{d/a} + \frac{7{,}34}{(d/a)^2}} \tag{5}$$

valid for $d/a \leq 4$ e $L/a \geq 5$, where d is the diameter (mm), the spacing between the probes (mm) and L is the length of the cylinder (mm). Thus, for the equipment with probe spacing of a = 37.5 mm or 50 mm, the geometric limits for applying the equation are $d \leq 150\ mm$ and $L \geq 187.5$ mm, which is met by the samples used, with nominal dimensions of 100 mm × 200 mm. The corrected resistivity is then:

$$\rho_{scorrigido} = \frac{\rho s}{k} \tag{6}$$

To avoid interference from different moisture contents, all the specimens were measured in a saturated surface dry condition. However, it is worth noting that the Spanish standard UNE 83988-2 [116] already recommends using shape factors to minimize the influence of sample geometry and electrode spacing.

Ultrasonic pulse velocity (UPV) was measured using 50 mm diameter transducers with a frequency of 54 kHz (Figure 5d). This non-destructive test is popular and is used to examine the homogeneity, quality, and presence of cracks, cavities, and defects in concrete. The time it takes for the wave to travel from one transmitting transducer to a receiving transducer through the specimen was measured. Using the height of each specimen and the average time measured, the ultrasonic wave propagation speed could be calculated for each sample.

Figure 5d shows the ultrasound pulse apparatus that was used to transmit and receive ultrasound waves through the cubes. The pitch-catch method was employed to record the time of arrival times as per ASTM C597 [113]. Pulses were generated by a pair of standard 54 kHz p-wave transducers that were held in contact with the specimen's surfaces. Because emitter technology is inexpensive, it is feasible to efficiently test a large number of specimens.

It should also be noted that the test was performed in a noise-free environment, as tracking performance can be affected by noisy. The UPV was measured by coupling of the transducers to the surfaces of the concrete cube in both saturated and dry states. For this experiment, the polymeric gel specified for the UPV testing was used as the coupling agent. It is main function was to facilitate transmission of ultrasound energy from the emitter to the concrete. Sufficient gel and pressure were applied to the surface of the cubes and the transducers to ensure stable transit times. Since the recorded results are mainly determined by access to the concrete surfaces, the transducers were located directly opposite each other. A direct transmission path was adopted for the best results. Figure 5d illustrates the location of the tested points.

Table 5 shows the parameters for evaluating concrete quality based on the propagation velocity of the ultrasonic wave, established by Cánovas [48].

3. RESULTS

3.1. Basic mechanical tests

Figure 6 presents the average and standard deviation results of the compressive strength tests.

Table 5: Relationship between concrete quality and UPV results, according to Cánovas [48].

UPV RESULTS (m/s)	CONCRETE QUALITY
UPV > 4,500	Excellent
3,500 < UPV < 4,500	Great
3,000 < UPV < 3,500	Good
2,000 < V < 3,000	Fair
V < 2,000	Poor

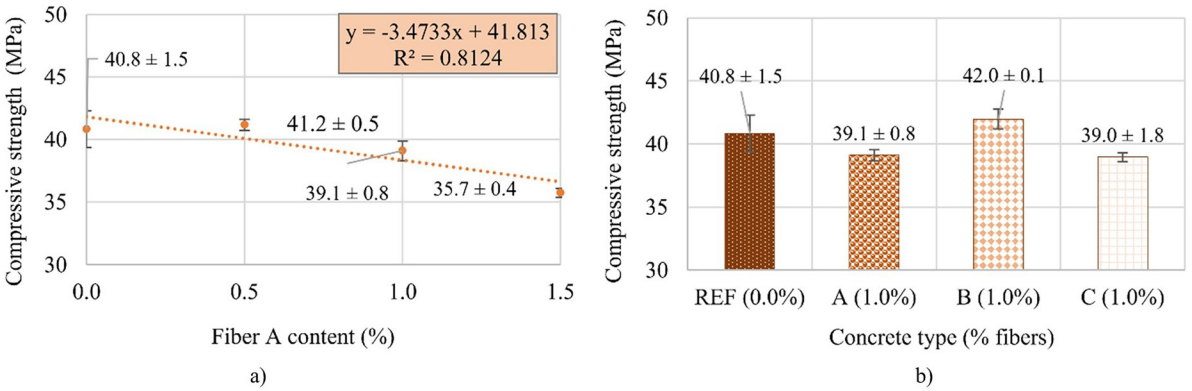

Figure 6: Compressive strength of concretes tested respect to (a) the content of fiber A, and (b) mixtures containing 1% of fibers A, B, and C, compared to the reference (without fibers).

Figure 6a shows a decreasing trend in concrete compressive strength values with an increase in the volume fraction (V_f) of Fiber A (copolymer). Concrete with a V_f of 1.5% exhibited 12.5% of reduction in strength compared to the reference. One potential explanation for the observed phenomenon could be the increase in fiber volume, which has been shown to result in the incorporation of additional porosity and voids within the matrix. This phenomenon can be quantified by the slight decrease in compressive strength. A general decreasing trend was observed, especially for higher fiber content. This behavior can be attributed to poor fiber dispersion and clumping ("balling effect") during the mixing process, as evidenced by this study. At the same time, an increase in water was observed with an increase in fiber amount (Table 4). This phenomenon can be attributed to an elevated water demand, resulting from the water absorption of fiber.

As demonstrated in Figure 6b, the fibers A and C resulted in a reduction of approximately 4% in the compressive strength when compared to the reference concrete. In contrast, fiber B concrete exhibited an approximate 3% increase. It is conceivable that this behavior is warranted on the basis that fibers A and C are monofilaments and do not possess irregular surfaces as compared to fiber B. Furthermore, the length (in millimeters) of fiber B exceeds than that of fibers A and B. This can modify the fiber aspect ratio and its adhesion to the matrix, effective fiber bridging, and properties associated with fiber pull-out, including chemical adhesion and frictional adhesion [1]. Additionally, a comparative analysis was conducted among concretes with fibers A, B, and C and the same V_f (1.0%), revealing that only the concrete devoid of fibers demonstrated a reduced w/c ratio. It is noteworthy that the other concretes possess an identical w/c ratio.

Indeed, the stress versus deformation response under compression load tests depends largely of the properties of the fibers, including their material, geometry, surface, stiffness, tensile strength, fiber volume fraction, shape, orientation, and distribution of the matrix, as well as the properties of the matrix and matrix-fiber interface [4, 12–16]. In certain instances, the presence of fibers has been observed to induce a stitching effect on cracks, thereby impeding their propagation and mitigating the ensuing damage under applied loads. Conversely, under certain circumstances they signify heterogeneous and vacuous zones.

A body of research has identified an increase in compressive strength with the incorporation of PP macro fibers [40, 77, 117–119]. Other results or reviews have indicated a decrease with polymeric and other types of fibers [41–43, 120–124]. As indicated in the extant literature, the length, distribution and the surface finish of the fibers have the capacity to exert an influence on compressive strength [1, 13, 14].

A one-way analysis of variance was conducted, taking into account two independent variables: concrete type (REF, A, B, and C) and fiber content (nested factor varying only for Fiber A) for the compressive strength test. The model demonstrated a significant result, as indicated by the calculated value of F and p-value ($F_{calculated}$ 14.048 > $F_{tabulated}$ 3.11 and value-p < 0), and yielded a coefficient of determination (R^2mod) of 0.854 and a coefficient of correlation (Rmod) of 0.924). Additionally, the concrete type (($F_{calculated}$ 9.43 > $F_{tabulated}$ 3.49) and fiber content (concrete type) ($F_{calculated}$ 21.00 > $F_{tabulated}$ 3.89) were found to be significant.

The incorporation of fibers into a concrete matrix signifies introduction of additional phases, thereby generating an increased number of interface regions and potentially resulting in heterogeneous zones characterized by the presence of gaps and voids. Consequently, of the material exhibits a decline with an increase in fiber content. In addition to fiber-matrix interactions, stress transfer, bond and pull-out, and fracture mechanics and interactions across cracks, other factors must be considered when assessing deformation and tension response under loads [4]. The effectiveness of fibers in enhancing the mechanical performance of the brittle matrix contingent, to

a considerable extent on the quality of fiber–matrix interactions. Three types of interactions must be considered: physical and chemical adhesion, friction and mechanical anchorage induced by deformations on the fiber surface or by overall complex geometry (e.g. crimps, hooks, deformed fibers) [4].

In the analysis of variance (ANOVA), the model obtained was representative (high R^2) , indicating that both factors analyzed were statistically significant and influenced the property under study. The fiber content was found to be the most significant factor. The significance of fiber content can be attributed to its impact on other concrete properties. The increase in fiber content, accompanied by a decrease in specific gravity, alters the workability due to the balling effect and the resultant trapping of free water [4, 12–16, 125].

This can result in elevated levels of porosity, thereby exerting an impact on the strength and durability of the material. This observation has been documented in other studies as well [124]. Thus, the porosity is increased, thereby affecting the durability of the concretes [4, 13, 14, 120]. In this research, workability of the concrete REF was maintained by increasing the FRC's water consumption, so increasing the water-to-binder ratio (minimum of 0.526 and maximum of 0.564) and, consequently, its porosity.

Furthermore, the multiple mean analysis test conducted by Duncan revealed that the concretes REF and C1.0B were in the same group, while the other two types of concrete (A1.0 and B1.0) were in a second group. This finding indicates that the data can be divided into two distinct categories. Additionally, Duncan's multiple mean analysis test was conducted, with the analysis limited to concretes containing fibers. This analysis resulted in the formation of two groups: one comprising concrete with fiber B, which exhibited an average of 42 MPa, and the other comprising concretes with fibers A and C, which both demonstrated average values of 39 MPa.

Another fundamental property was the modulus of elasticity, the results of which are presented in Figure 7.

As demonstrated in Figure 7, the outcomes for varying proportions of fiber A exhibited a declining trend as the fiber content increased, attaining a 11.2% disparity between REF concrete and C1.5A. This decrease in the modulus of elasticity is attributable to the lower elastic modulus of the polypropylene fibers in comparison to the cementitious matrix. This finding is consistent with observations from other studies [12, 123]. The incorporation of plastic fibers with a low elastic modulus (5–10 GPa) into a concrete matrix has been shown to have a detrimental effect on the overall modulus of elasticity [112]. As illustrated in Figure 7b, the incorporation of fiber into the concrete resulted in a decline in outcomes, with a maximum of 18.7% achieved using Fiber B.

3.2. Flexural tensile strength

Figure 8 shows the load vs. crack opening diagrams for the samples tested.

From the diagram in Figure 8a, comparing the FRC with Fiber A to the reference concrete (without fiber), it can be seen how the addition of polypropylene fibers improves the flexural response of the cementitious matrix. The reference concrete samples broke before the test ended (Figure 9a) with a maximum deformation of 1.88 mm, while the FRCs exceeded 4 mm of CMOD, supporting more load than the REF concrete and did not break as shown in Figures 9b to 9d. This indicated that the polypropylene macro fibers distributed the tensile forces and mitigated the crack propagation [112].

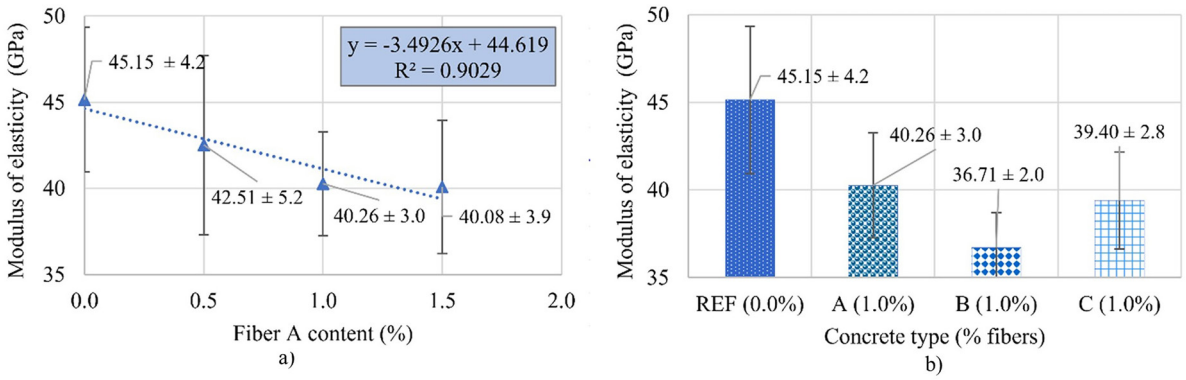

Figure 7: Modulus of elasticity of the concretes tested *versus* (a) fiber A content and (b) Fiber A, B and C with V_f of 1.0%, compared to the reference.

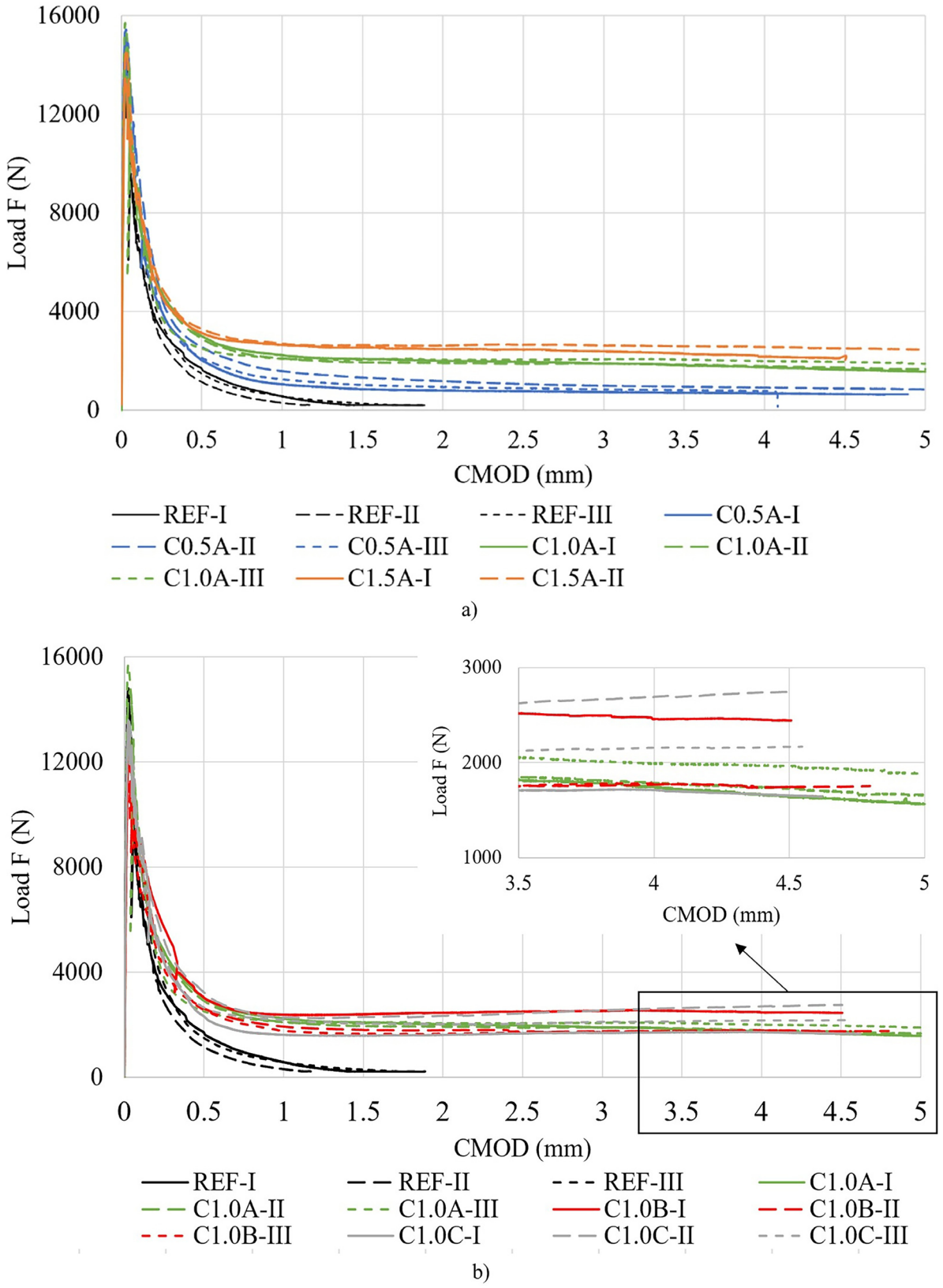

Figure 8: Flexural tensile strength test: load CMOD diagrams for the reference concrete and the concretes with: (a) varying fiber A content (from 0% to 1.5%) and fibers A, B and C at the 1.0% (V_f).

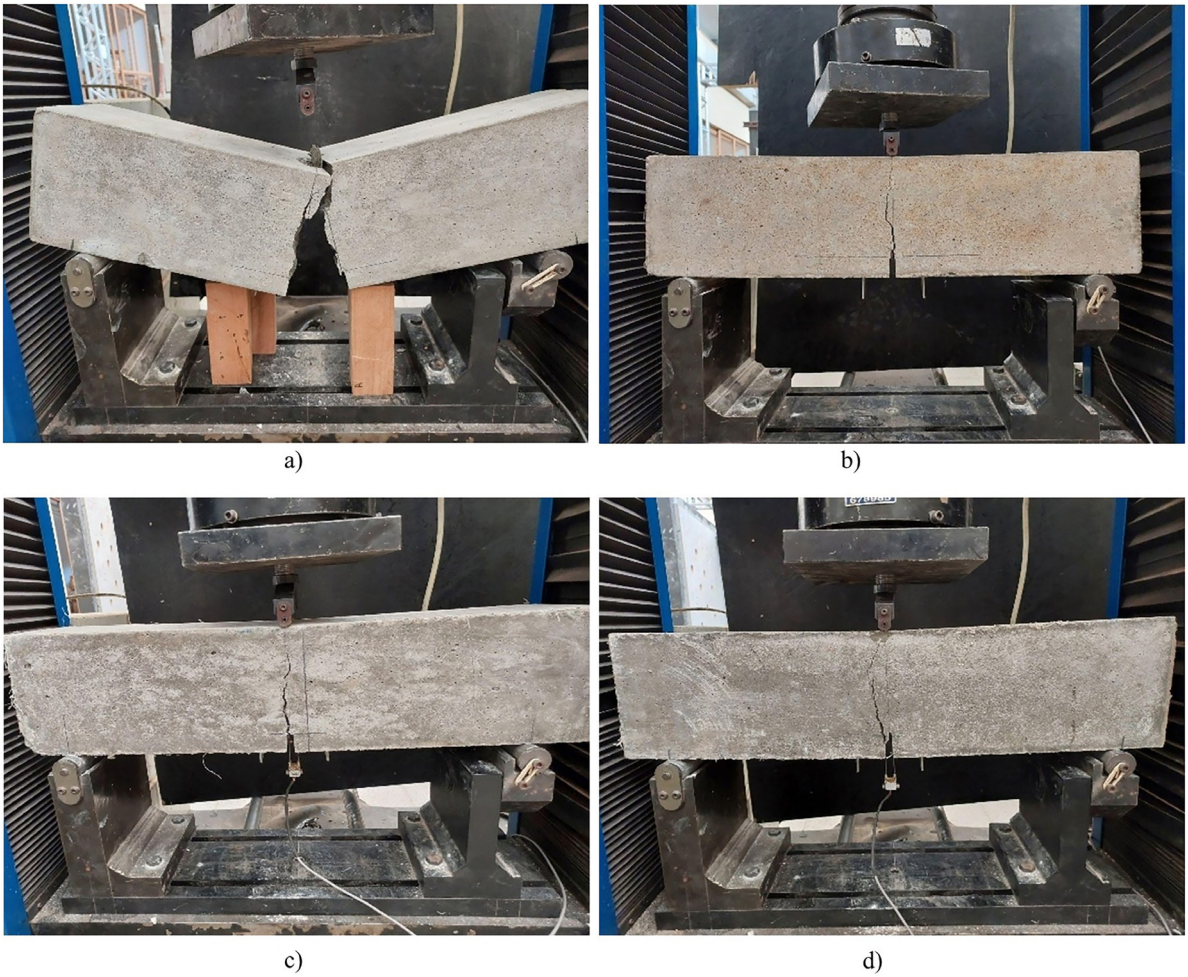

Figure 9: Final stage of the flexural tensile strength tests for the concretes: (a) REF, (b) C0.5A, (c) C1.0A, and (d) C1.5A.

In Figure 8b, comparing the FRCs with 1% addition (Fibers A, B, and C) to the concrete REF, it was observed that the addition of any fiber improved the flexural response of the cementitious matrix. Analyzing the type of fiber used, a similar behavior was observed between them.

The tendency shown in the graphs, with a sharp drop after the peak load (limit of proportionality), is a typical strain-softening behavior, where the load-bearing capacity decreases as crack openings increase. The increase in the addition content of Fiber A increased the load-bearing capacity of the material (Figure 9).

From the diagram data and sample measurements using Equations 1 and 2, the limit of proportionality (LOP) and residual flexural tensile strengths (fR1 to fR4) were calculated, as presented in Table 6 and Figure 10. From the results of the flexural tensile strength test, the limits of proportionality of the concretes were calculated.

Regarding the limit of proportionality (Table 6), corresponding to the maximum flexural tensile strength of the concretes, the values were close, with a slight tendency for the fL to increase as the fiber A content increased, considering the average. However, when considering the standard deviation, the value remained practically constant. This is because the opening of the first crack is more closely related to the properties of the cementitious matrix than to those of the fiber. Since the matrix was kept constant, the addition of type A macro fibers had no effect on the LOP. However, with the addition of fibers B and C, there was a reduction in LOP with respect to both the reference concrete and the concretes with fiber A.

In terms of residual strength (Figure 10a), the FRCs with fiber A performed significantly better than the concrete REF. For fR1 (CMOD = 0.5 mm), the strength increased up to 136% for the C1.5A concrete, and for fR2 (CMOD = 1.5 mm), the increase was 1157%. The increase in fiber content resulted in an increase in residual strength. This indicates that the incorporation of fibers into the concrete increased its toughness and ductility and reduced its fragility.

When comparing the fiber types for the same content (Figure 10b), it was observed that the residual strengths were close and considering the standard deviations, they can be considered similar. Although concrete

Table 6: Limit of proportionality of the concretes and parameters from fib Model Code 2010 [125].

CONCRETE	FL (MPA)			PARAMETERS OF FIB MODEL CODE 2010 [125]		
	AVERAGE (MPa)	STANDARD DEVIATION (MPa)	COEFFICIENT OF VARIATION (%)	FR3/FR1	FR1/FL	CLASSIFICATION
REF	4.50	0.08	2%	–	–	–
C0.5A	4.60	0.34	7%	0.406	0.152	–
C1.0A	4.62	0.22	5%	0.708	0.193	B
C1.5A	4.71	0.41	9%	0.796	0.229	B
C1.0B	4.01	0.15	4%	0.717	0.223	B
C1.0C	4.16	0.10	2%	0.737	0.205	B

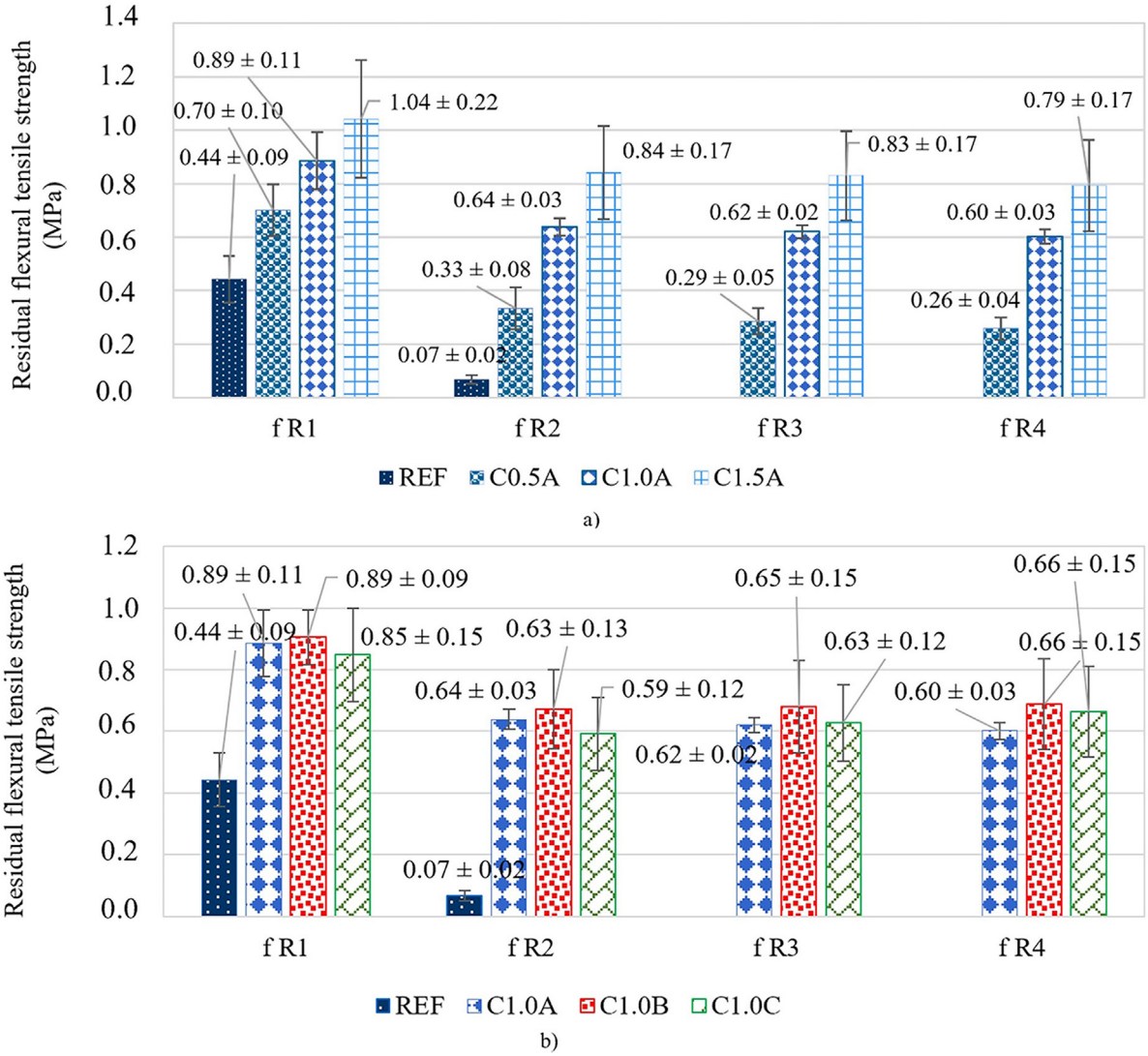

Figure 10: Residual flexural tensile strengths for the reference concrete and concretes with: (a) varying dosages of fiber A, and (b) for concretes with 1% of fibers A, B, and C.

C1.0B and C1.0C had a lower limit of proportionality than concrete C1.0A, their residual strengths were very close.

MONTEIRO *et al.* [126] studied the mechanical behavior of steel, polypropylene, and hybrid FRCs by performing the flexural tensile strength test according to EN 14651 [81]. In contrast to this research, the matrix had mineral additives such as silica fume and fly ash, and the polypropylene fibers were 40 mm long, with a consumption of 3, 6 or 10 kg/m^3 of concrete. The behavior of these authors' polypropylene FRCs generally showed the same trend as this research (strain-softening), but maintaining a more constant residual strength, for the C1.5A equivalent mix.

To assess the impact of fiber type and content on the residual tensile strength, an analysis of variance (ANOVA) was conducted on the fR3 strength values (CMOD = 2.5 mm). The model demonstrated a high degree of significance, as evidenced by the calculated value of 10.521, which exceeds the tabulated value of 3.63. This finding indicates that the model has a strong explanatory power, as indicated by the coefficient of determination (R^2_(mod)) of 0.824 and the coefficient of correlation (R^2_(mod)) of 0.908. Additionally, the fiber type was not found to be statistically significant (F calculated = 0.62 > F tabulated = 4.26). However, the fiber content was determined to be statistically significant (F calculated = 19.59 > F tabulated = 4.26).

The analysis of variance (ANOVA) revealed that the presence of fiber A was found to be statistically significant. This finding indicates that the content of fiber A exerts a substantial influence on the residual strength, as evidenced by a representative model that exhibits a high coefficient of determination. However, the fiber type was not found to be a significant factor. Consequently, in Duncan's test, all the concretes with 1.0% fiber (1.0A; 1.0B and 1.0C) were placed in a single group, and each of the other contents (0.5A and 1.5A) were placed in a different group.

As illustrated in Table 5, the results of the concrete utilized in this study are also presented for the classification parameters proposed by the fib Model Code 2010 [125]. The ratio between fR3 and fR1 is a critical metric for the classification of concrete in terms of its residual strength. Concretes C1.0A, C1.5A, C1.0B, and C1.0C are classified as Class B. According to the criteria outlined in this code, the incorporation of fiber reinforcement has the potential to substitute for conventional reinforcement in the ultimate limit state (ULS) under certain conditions. Specifically, the presence of two conditions is requisite: fR1/fL must exceed 0.40, and fR3/fR1 must surpass 0.5. The initial condition is not satisfied, as the concrete strengths in this study rapidly decrease following the formation of the initial crack. Consequently, as per the aforementioned criteria, the FRCs examined were found to be inadequate in replacing the conventional reinforcement in the ULS.

Despite the fact that fiber-reinforced concretes do not comply with the fib Model Code 2010 [125] criteria for total reinforcement replacement in the ultimate limit state (ULS), the residual flexural strength results indicate significant gains in toughness and post-cracking behavior. These gains are particularly relevant in applications where crack control and ductility are paramount, such as in industrial flooring and pavement construction. Research has demonstrated a direct correlation between the type and volume fraction of fibers and the residual mechanical performance of the material [4, 14, 15, 120].

3.3. Non-destructive tests

The results of the resistivity excluding the application of any correction factors, are presented in Figure 11a. This figure illustrates the uncorrected values of SEM 50 mm and SEM 38, along with the bulk resistivity). The values of k, as determined by equation 4 are 3.27 and 2.35 for the respective SEM 38 mm and 50 mm measurements. The SEM values that have undergone correction via by equation 5 are displayed in Figure 11b.

In general, as demonstrated in Figure 11a there was a tendency for surface electrical resistivity (SER) values when not corrected for SEM 50 mm and SEM 38 mm, to exceed bulk resistivity (BR) values. This tendency remained consistent irrespective of the presence, type, and content of fibers (Vf). This same tendency was observed for concretes with other compositions and porosities, but without fibers [46, 64, 66]. The extant literature indicates that the probe spacing employed in surface resistivity readings, or readings obtained with probes embedded in concrete specimens, can serve as a significant variable in Re tests, with a lower degree of significance than the concrete type. Consequently, it is imperative to consider this aspect when comparing results obtained by disparate devices and equipment [66] and correction factors [125, 127].

It has been demonstrated that probe spacings of a reduced dimension tend to measure real values from layers of a more superficial nature and in closer proximity to the concrete cover region. It has been demonstrated that larger probe spacings tend to express Re values from deeper layers of the concrete. Volumetric or bulk Re is a method of measuring the specimen's overall resistivity from top to bottom. This approach ensures a more reliable analysis of the material's overall property, as it reduces the impact of surface defects or carbonation and accounts for the interference of aggregates (primarily coarse ones) in this process [66]. For all

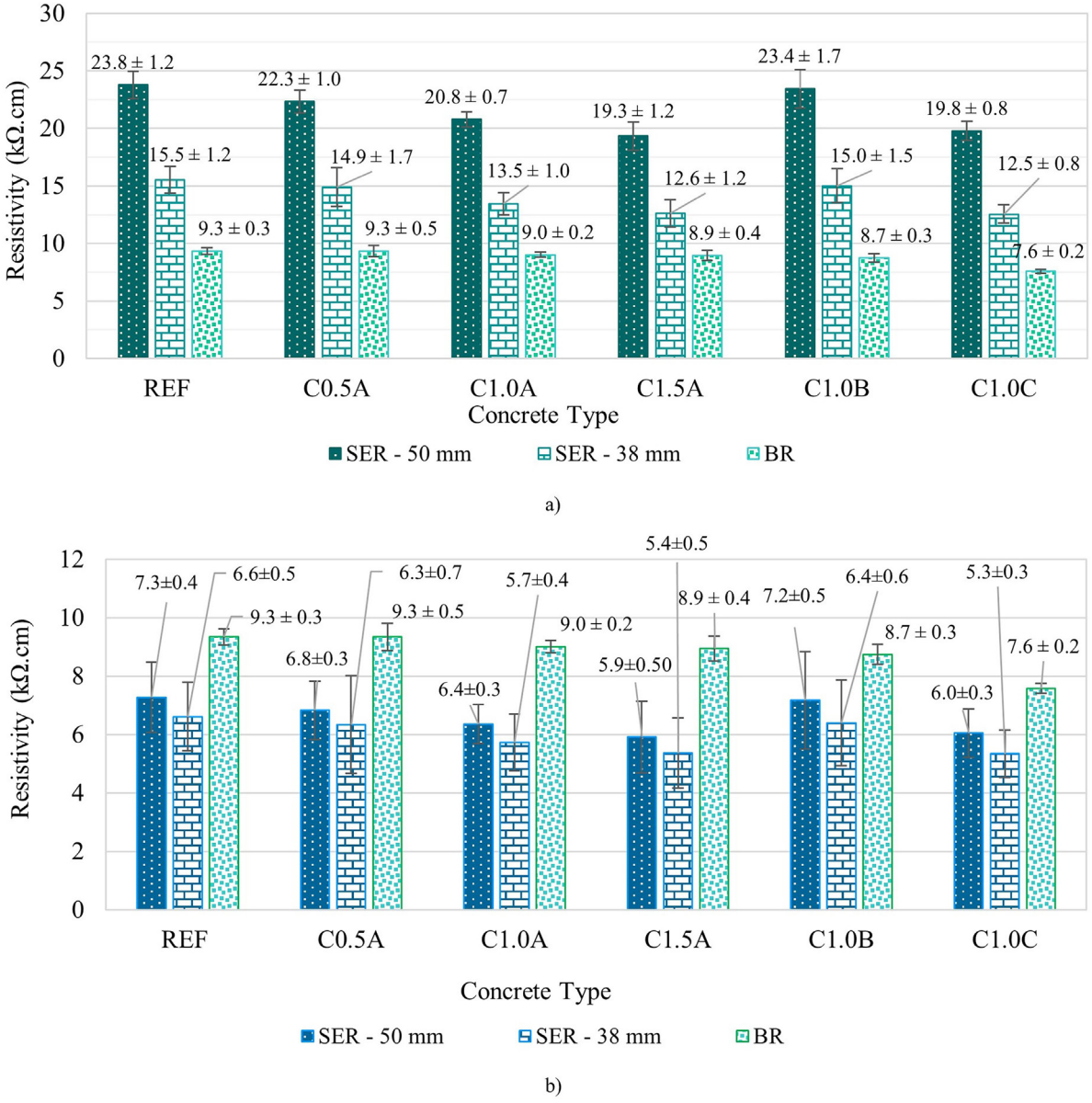

Figure 11: Surface and bulk resistivities for all types of concrete studied: (a) resistivity without applying correction factor for SER 50 mm and SER 38 mm, and (b) resistivity with correction factors applied according to the specimen geometry.

concretes examined, in descending order of values, the values of Bulk, SEM 50, and SEM 38 were obtained (see Figure 11b). Therefore, the resistivity values obtained using different devices exhibited variations, yet demonstrated a consistent decreasing trend.

It is imperative to ensure the accuracy of resistivity values by utilizing geometry specimens [127]. Figure 11b demonstrates a decline in SER and BR values with an increase in fiber A content in the concretes. The concrete reference exhibited significant SER and BR values among the concretes examined. This concrete has the lowest water-to-binder ratio in comparison to other concretes. Concretes with higher compacity and lower paste porosity demonstrate the highest values of electrical resistivity. This behavior was reflected in the compressive strength. Therefore, the higher resistivity is the result of physical changes in cement paste, including pore refinement and densification of the internal structure of concrete [73, 74, 128]. These changes may also be due to chemical changes in pore solution. The resistivity is a critical parameter for assessing the durability of concretes, particularly in structures exposed to ion attack, such as those affected by chlorides in marine atmospheres [128]. According to the SER criterion, concretes can be classified as having high probability of corrosion [71].

The potential explanations for the observed phenomenon include the hypothesis that the augmentation in fiber volume may have concomitantly entailed an escalation in porosity and void content within the matrix.

This hypothesis is predicated on the premise that the slight diminution in compressive strength can be attributed to these porosity and void-related phenomena. In general, especially for higher fiber content, a decreasing trend can be observed due to the poor dispersion of fibers and the formation of clumps of fibers ("balling effect") during the mixing process, as in the case of this study. Concurrently, an increase in water was observed with an increase in fiber (see Table 4). This phenomenon can be attributed to the elevated water demand resulting from fiber absorption (see Table 4).

A comparative analysis reveals that concrete containing 1.0% of fiber B exhibits the highest SER values, followed by concretes with fibers A and C. In these concretes, the ratio of water to binder remained constant. It is possible that this behavior is justified because fibers A and C are monofilaments and do not have irregular surfaces as compared to fiber B. Furthermore, the length (in millimeters) of fiber B is greater than that of fibers A and B. This can change the fiber aspect ratio and its adhesion to the matrix, effective fiber bridging, and properties related to fiber pull-out, as chemical adhesion and frictional adhesion [4].

The present study examined the relationship between the fiber content (1%) and the bulk resistivity, observing a decrease in resistivity with alterations in fiber A, B, and C. This phenomenon may be attributed to the dispersion and homogenization of the fibers within the matrix.

The stress versus deformation response under compression load tests is contingent on the properties of the fibers, including their material, geometry, surface, stiffness, tensile strength, fiber volume fraction, shape, orientation, and distribution of the matrix, as well as the properties of the matrix and matrix-fiber interface [4, 13, 14]. In certain instances, the presence of fibers has been observed to induce a stitching effect on cracks, thereby impeding their propagation and mitigating the ensuing damage under applied loads. Conversely, under certain circumstances, they manifest as heterogeneous and unoccupied zones. This phenomenon could be indicative of an increase in the concrete's porosity with the incorporation of fibers and an increase in the water-to-cement ratio. These findings align with the observed trends in compressive strength and modulus of elasticity, thereby substantiating the reliability of the experimental approach. Additionally, the incorporation of fibers was observed in all resistivity types that were examined, with the general trend indicating a reduction in resistivity, with the exception of types B and SEM 50. Despite the variation in water content, the concretes incorporating fibers exhibited a propensity to decrease the values of all measured resistivities (from SEM 50 to SEM 38 mm).

The incorporation of additional phases, namely fibers and fiber-matrix interfaces, has been shown to suggest a detrimental tendency Re, which can modify crucial aspects of concrete durability, including its mass transport properties and its resistance to chloride penetration. However, the beneficial effect of fibers on durability is evident under loads and on the phenomenon of controlled cracking. Specifically, fibers have been shown to maintain crack openings (width) of small diameter and little spacing between them. In some cases, these apertures have been observed to measure approximately 30 to 40 micrometers in diameter [129]. With regard to bulk resistance, the values of all the concretes studied exhibited minimal variation, with a maximum reduction of 4.6%. Furthermore, studies have investigated mortars with conductive properties, obtained by incorporating materials such as single-walled carbon nanotubes and metal fibers. These studies have demonstrated that electrical resistivity is influenced by the conductive nature of the incorporated reinforcements, the homogeneity of the dispersion, and the connectivity of the conductive network formed in the cementitious matrix [123].

The Spanish coefficients obtained by standard UNE 83988-2 [116] for minimizing the influence of specimen geometry and electrode spacing were 0.377 for SEM 50 mm and 0.571 for SEM 37.5 mm. As illustrated in Figure 12, the relationship between SEM measurement (kohm.cm), corrected by EN UNE 83988-2 [116], and SEM measurement corrected by [115], is demonstrated (Figure 12).

A strong correlation was observed between resistivity values (kohm.cm) that were rectified using EN UNE 83988-2 [116] and those that were modified using SEM measurement (kohm.cm), corrected by EN UNE 83988-2 [116], and SEM measurement [115]. The R-square values were 1.0, but with different values for SEM 38 mm and SEM 50 mm.

The compressive strength was found to be correlated with Bulk, SEM 38 mm and SEM 50 mm, as previously established by [115] (see Figure 13).

Regardless of resistivity type, excellent linear correlations were observed., However, it is important to acknowledge the limitations of the study, which included a relatively small sample size and a limited variety of concrete types. In other studies, researchers employed a logarithmic approach to analyze the correlation between electrical resistivity and compressive strength of concrete devoid of fibers (R-Squared over 0.98) [72].

The relationship between the two parameters was direct and proportional; that is to say, as the compressive strength increased, the electrical resistivity also increased [72–74]. A number of studies have been conducted on the correlation between compressive strength and surface electrical resistivity of concrete, as well

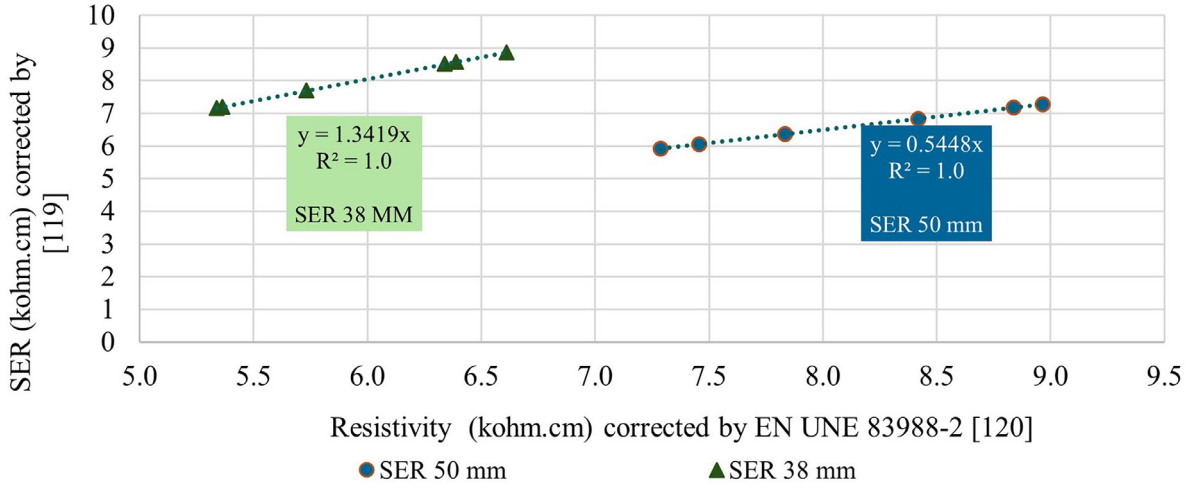

Figure 12: Relation between resistivity values (kΩ.cm) corrected according to EN UNE 83988-2 [116] and SEM corrected according to [115] for SEM 50 mm and SEM 38 mm.

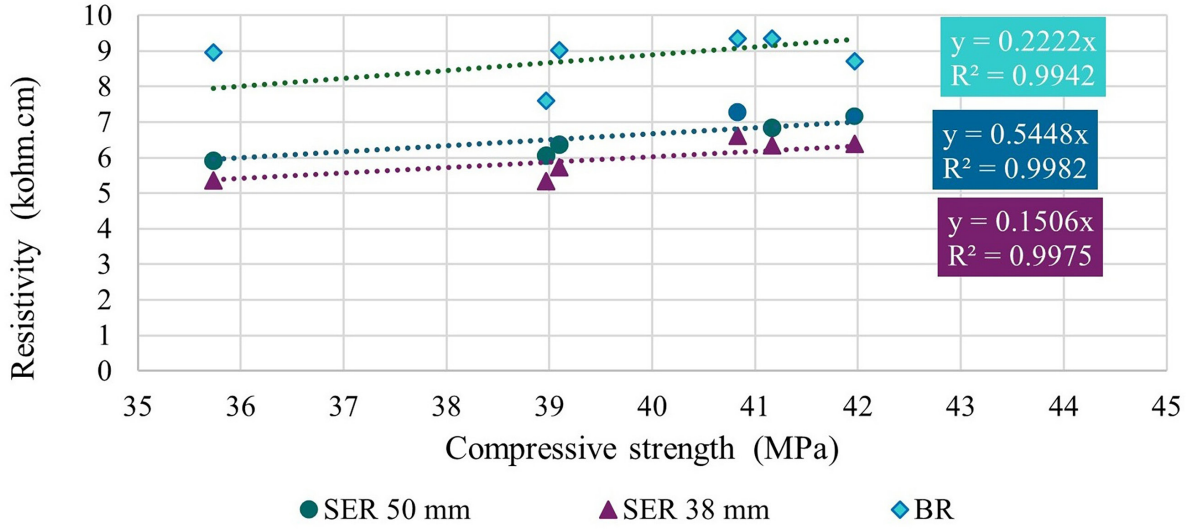

Figure 13: Correlation between compressive strength and resistivity for the concrete tested.

as between splitting tensile strength and surface electrical resistivity of Brazilian concretes devoid of fibers. The following general relationships are observed: $fc = 14.18 \cdot \ln(\rho) + 18.43$ and $ft = 0.69 \cdot \ln(\rho) + 2.15$. The first relationship is applicable to compressive strength, while the second is applicable to splitting tensile strength. In the context of these studies, the concrete specimens were not reinforced with fibers [75]. The present study found no correlation between flexural strength and resistivity values, nor between resistivity values and modulus of elasticity.

In the case of concrete with fibers, the presence of fibers, in conjunction with their type and content, has the capacity to modify the electrical resistivity values of cementitious materials. A study was conducted by some authors [76] on the electrical resistivity of various mortars incorporating carbon and PVA (polyvinyl alcohol) fibers. The mortars comprising solely PVA fibers exhibited significantly higher resistivity in comparison to those consisting of than the materials with only carbon fibers. Moreover, an increase of the PVA fiber content resulted in a decrease in resistivity. In another study, [77] the electrical resistivity of concrete was analyzed with conductive fibers (steel fibers) and non-conductive fibers (macro-polypropylene, micro-polypropylene, and micro nylon), with and without silica fume. The results demonstrated a modest decrease in bulk resistivity following the incorporation of non-conductive fibers into plain concrete, accompanied by a negligible change in surface resistivity.

In addition, an investigation was conducted to ascertain the impact of V_f (ranging from 0% to 1.5% copolymeric fiber) on the BR. This investigation employed a one-way analysis of variance (ANOVA) statistical approach as a methodological framework. The model demonstrated a significant result ($F_{calculated}$ 3.098 > $F_{tabulated}$ 2.90). However, the coefficient of determination (R^2_(mod)) and the coefficient of correlation (R_(mod)) were found to be 0.255 and 0.474, respectively. Conversely, the impact of fiber type on the BR demonstrates that the model was statistically significant ($F_{calculated}$ = 79.070 > $F_{tabulated}$ = 2.90) with a coefficient of determination (R2mod) of 0.881 and a coefficient of correlation (R_{mod}) of 0.939. The fiber type proved to be a significant variable in the BR. Accordingly, the Duncan test displays the mean values for each type of V_f of the FRC studied (0%, A, B, and C).

As illustrated in Figure 14, the ultrasonic pulse velocity results for the studied concretes presented. An increase in the number of fibers can lead to alterations in the velocity of ultrasonic wave propagation. These alterations can be attributed to the formation of voids and/or clumping. Indeed, although large volumes of fiber are desirable from the point of view of improving mechanical behavior, practical application limitations may occur with larger volumes of fibers (greater than 2%) from the point of view of mixing, workability, molding, and compaction of fibrous concretes [4, 13, 14, 36].

A decrease in the mean value of the UPV was observed in Figure 14a, accompanied by minimal variability, as the V_f increased. The variation between the reference concrete and those with varying additions of Fiber A (100% pure copolymer) was minimal, with a difference from 0.9% to 1.6%. These values correspond to the respective concretes 0.0% (ref), 0.5%, 1.0%, and 1.5%, respectively. This variation in results is indicative of the inherent inconsistencies in the data. A review of the extant literature reveals a consistency in the findings, with studies demonstrating a decrease in ultrasonic velocity as the steel volume fraction increases [49], and decreases in ultrasonic velocity for various fibers, including nylon, polypropylene, stainless steel, and glass [51], as well as PVA fibers [130, 131].

The UPV exhibited an increase concomitant with the rise of V_f. This phenomenon manifested in comparison to the reference concrete value established. The potential for this occurrence may be attributable to the incorporation of mineral additions, such as silica fume and fly ash into to the matrix. The experimental findings indicated that UPV was 2,650 m/s for the concrete without fibers, while the UPV on the concrete with fibers was 4,900 m/s.

As indicated by the research ultrasonic pulse velocity (UPV) tests had been performed to evaluate the internal integrity, homogeneity, and density variations of concrete samples. The presence of polypropylene macrofibers has been demonstrated affect wave propagation by introducing discontinuities or increasing porosity due to fiber dispersion, especially at higher volumes. The presence of these changes can be detected through variations in UPV values. Previous studies have demonstrated a correlation between these variations and the presence and distribution of fibers in the concrete matrix [132].

In consideration of the comparison of V_f (1.0%) (Figure 14b), the C1.0B concrete (with polyethylene/polypropylene fibers) exhibited a marginally elevated velocity in comparison to the other specimens (1.8% compared to REF), aligning with the observed trend in the preceding test.

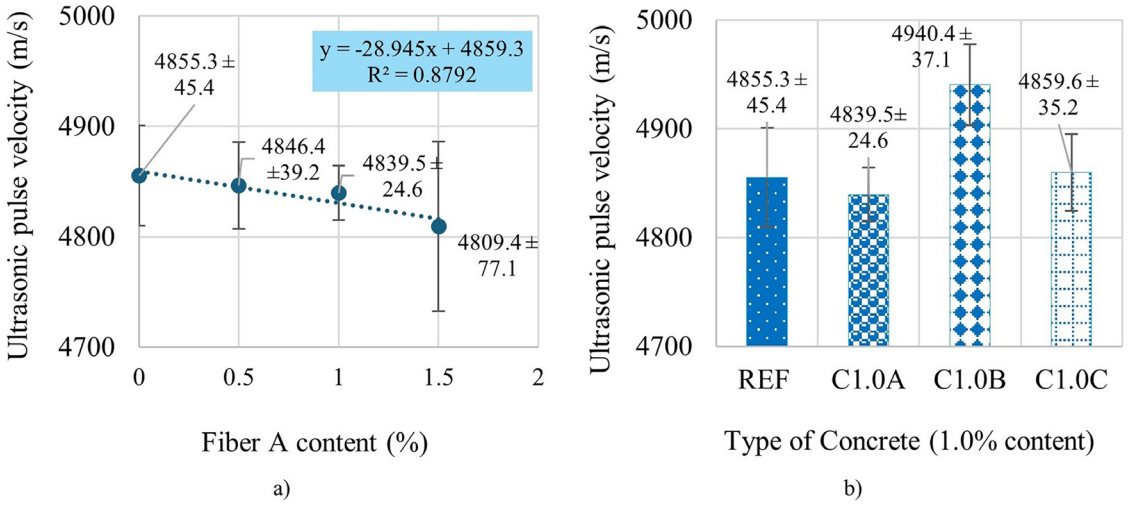

Figure 14: Average and standard deviation of ultrasonic pulse for the reference concrete and concretes reinforced with: (a) fiber A, and (b) fibers at 1.0% V_f.

The UPV value exhibited minimal sensitivity to the incorporation of fibers; however, it demonstrated discernible sensitivity to variations in compressive strength values. All the concretes examined were classified as excellent quality by Cánovas [81]. The present study demonstrated a strong correlation between UPV and compressive strength (R^2 = 0.9979) (see Figure 15), as well as between UPV and modulus of elasticity (see Figure 16). Additionally, a correlation was observed between UPV and modulus of elasticity in GPa. In the extant literature, strong positive correlations with R^2 values greater than 0.90 have been documented for concretes devoid of fibers and various types of cements [72] as well as for concretes containing fibers. An increasing trend was observed in the plot of compressive strength as a function of UPV, concurrent with the increase in the alkali content of geopolymer mortars. The slope values exhibited a strongly related linear function relation with R^2 values ranging from 0.87 to 0.96 and flexural strength values ranging from 0.94 to 1.00 [133]. As indicated by the findings of [140], the correlations between UPV and flexural strength were considerably weaker, with R^2 values ranging from 0.0036 to 0.712.

A clear exponential correlation between UPV and compressive strength was observed for concrete reinforced with polyvinyl alcohol (PVA) fibers [134]. In contrast, the correlation between UPV and flexural strength exhibited considerably weaker associations, with R^2 values ranging from 0.0036 to 0.712 [134]. This scatter could be attributed to variability resulting from the combined influence of crumb rubber particles and PVA fibers. The weaker correlation observed for flexural strength in comparison to compressive strength is likely attributable to localized fiber-induced crack-bridging effects, which may not be adequately captured by UPV measurements [134].

The effect of V_f (from 0% to 1.5% copolymeric fiber) on the UPV was investigated through the utilization of a one-way analysis of variance (ANOVA) statistical approach. However, this approach yielded a coefficient of determination (R^2mod) of 0.235 and a coefficient of correlation (Rmod) of 0.485). Also, the impact of the fiber type on the UPV was examined. The model demonstrated a significant result ($F_{calculated}$ 5.887 > $F_{tabulated}$ 2.91) with a coefficient of determination (R^2mod) of 0.363 and a coefficient of correlation (Rmod) of 0.602).

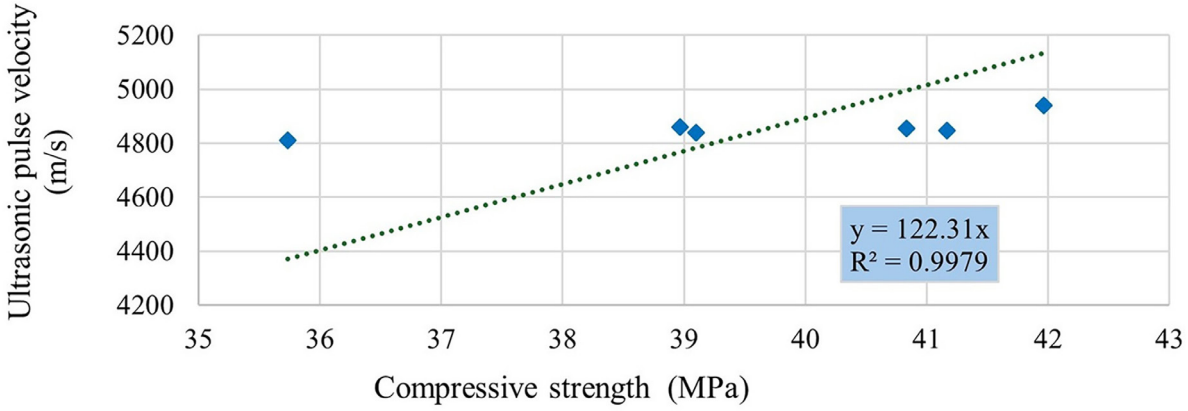

Figure 15: Correlation between compressive strength (MPa) and ultrasonic pulse velocity - UPV (m/s).

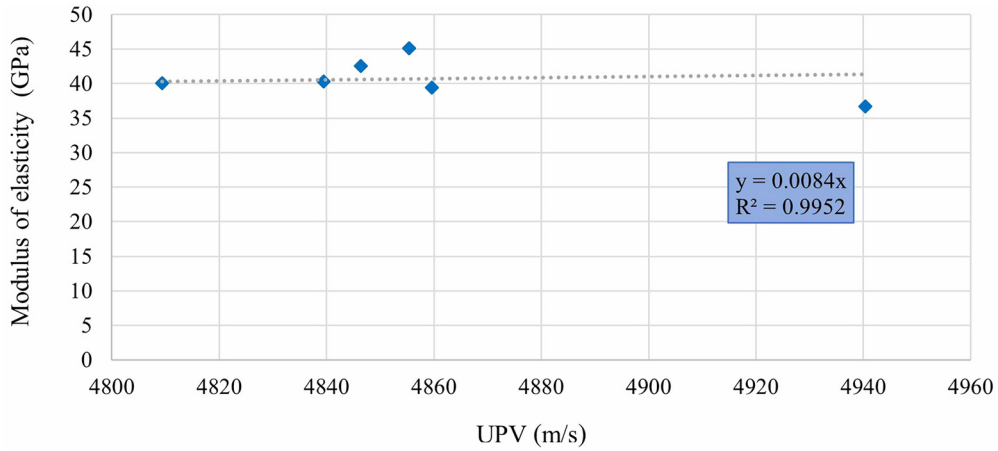

Figure 16: Correlation between ultrasonic pulse velocity - UPV (m/s) and modulus of elasticity (GPa).

The present study examined the relationship between the reinforcement index (RI) and the mechanical properties of concretes containing polypropylene fibers in various volumes (0, 0.4, 0.8, and 1.2%) and lengths (40, 50, and 60 mm). The results demonstrated a linear correlation between the RI and the mechanical properties, with a correlation coefficient of 0.79. An increase in the RI corresponds to a decrease in the compressive strength. The findings indicate an absence of a correlation between IR and the Static Modulus of Elasticity, even when the correlation coefficient reaches 0.47. This observation suggests that the Static Modulus of Elasticity remains largely uninfluenced by PP fibers. Consequently, conventional concrete formulas can be employed to calculate its value, irrespective of the presence of reinforcing fibers. This conclusion holds true for PP fiber volume fractions ranging from 0% to 1.2% [135].

The correlation between the reinforcement index and ultrasonic pulse velocity, as determined by the three prospecting methods, is indicative of a relationship between the variables. Conversely, an increase in the RI is associated with an increase in the UPV. However, a significant correlation was identified only through the indirect method regarding the relationship between the dynamic modulus of elasticity and RI. The correlation between dynamic and mechanical properties is significant. There is a strong relationship between UPV and compressive strength, as well as between UPV and the static modulus of elasticity. In both cases, the indirect prospecting method was the sole method that demonstrated a significant correlation. Consequently, empirical equations have been developed to represent these relations. In the initial instance, an elevated UPV is associated with diminished compressive strength, as evidenced by a correlation coefficient of 0.64. In the second case, the correlation coefficient between the UPV and the static modulus of elasticity is 0.68, indicating a direct relationship between the two parameters. Conversely, a correlation has been demonstrated between the dynamic modulus of elasticity and compressive strength. However, this correlation does not extend to the static modulus of elasticity. Therefore, a correlation equation of the dynamic modulus of elasticity with compressive strength and RI has been developed [135].

The volumetric resistivity exhibited no linear or logarithmic correlation with UPV; rather, it demonstrated a degree 3 polynomial relationship.

4. DISCUSSION

The incorporation of fibers into the concrete specimens examined typically led to a diminution in the concrete's compressive strength and modulus of elasticity. However, a substantial enhancement in its flexural tensile strength was observed subsequent to cracking. The incorporation of fibers into the cementitious matrix enhanced its ductility. This enhancement is attributed to the action of polypropylene fibers, which function as bridges between cracks, thereby impeding crack growth [118].

To corroborate this analysis, the graph in Figure 17 presents the fracture energy of the concretes. The incorporation of fibers has been demonstrated to result in a substantial increase in energy, ranging from 152% to 369% compared to concrete REF. The fracture energy is the primary parameter that governs the damage and fracture mechanisms [136]. It is defined as the total energy required for the rupture of a unit area of concrete fracture ligament [137]. The enhancement in fracture energy can be attributed to the crack-bridging effect of the

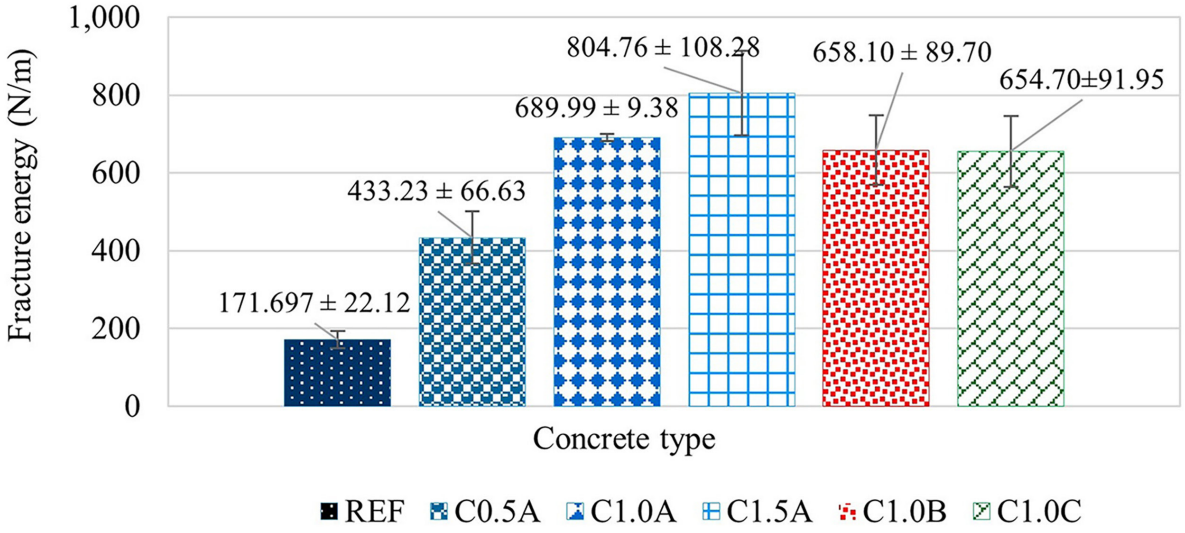

Figure 17: Fracture energy of all concretes.

PP fibers. The presence of multiple post-failure cracks, as well as a reduction in the brittle failure mechanism characteristic of the cementitious matrix, have been observed [118]. As anticipated, an increase in the content of fiber A resulted in an observable rise in energy levels during the observation of concretes. A comparison of various fibers revealed that concrete C1.0A exhibited a higher fracture energy.

A comprehensive analysis of the conducted tests revealed that Fiber A exhibited the optimal overall performance at a mass percentage of 1%, corresponding to a fractional volume of 3.35%. Concrete C1.5A demonstrated a 34% increase in residual flexural strength compared to C1.0A. However, its classification according to the parameters of the Fib Model Code [125] remained unchanged (class B), and its performance in the other tests was lower than that of C1.0A concrete. Therefore, it can be concluded that C1.0A concrete is a more economical concrete than C1.5A. This is due to the fact that C1.0A improves the tensile performance compared to REF concrete, with only small or insignificant losses in other properties.

An evaluation of the three fibers utilized, each with a fixed content of 1%, revealed a generally similar behavioral pattern. Concrete with fiber B demonstrated superior performance in non-destructive tests and compressive strength. In the flexural tensile test, C1.0A concrete exhibited higher LOP and fracture energy.

Some interesting correlations were observed between destructive and non-destructive tests. A greater volume of fibers can result in a slower speed of propagation of ultrasonic waves. This was noted on the Figure 14. At the same time, the material, geometry and shape of the fibers can affect how they disperse and distribute in the cementitious matrix. This seems to be reflected in the propagation speed of ultrasonic waves, as shown in Figure 14b. Therefore, the Fiber B with irregularities on their surface allowed better adhesion to the matrix, resulting in higher ultrasonic wave speeds in the concrete. In this study, second UPV results, the geometry of fiber had influenced more than the type of material of fiber.

A number of noteworthy correlations were identified between destructive and non-destructive testing methods. An increase in the number of fibers present can lead to a reduction in the velocity of ultrasonic wave propagation. This observation is corroborated by Figure 14. Concurrently, the material, geometry, and shape of the fibers can influence their dispersion and distribution within the cementitious matrix. This phenomenon is exemplified by the propagation speed of ultrasonic waves, as demonstrated in Figure 14b. Therefore, the presence of irregularities on the surface of Fiber B facilitated enhanced adhesion to the matrix, thereby resulting in elevated ultrasonic wave speeds within the concrete. The present study's findings, which are consistent with those of the second UPV study, indicate that the geometry of the fiber is a more significant factor than the type of material used in determining the outcome.

There are correlations between compressive strength and resistivity. The SER and bulk resistivity increase, the compressive strength increases, probably because these two properties are influenced by the porosity and microstructure of the cementitious matrix. It is known that electrical resistivity readings taken at different probe spacings and with probes embedded in concrete specimens can significantly affect Re test results, with a lower degree of significance than the type of concrete. Therefore, it is necessary to take this into account when comparing results obtained using different devices and equipment [46, 53, 66, 72].

An interesting result is that the UPV technique was sensitive to expressing changes in volume and different fiber materials/geometries into the concretes studied and their compressive strength.

Regarding the flexural tensile test, the best correlation with the non-destructive tests was the limit of proportionality with the ultrasonic pulse velocity. The correlation was inversely proportional, which is contrary to expectations since higher velocity values generally indicate more compact cementitious matrices. Then, a relationship was established between the limit of proportionality (MPa) and UPV - ultrasonic pulse velocity (m/s) for the (Equation 7), with an R^2 value of 0.7644.

$$\text{Ultrasonic pulse velocity value} = -136.59 \text{ limit of proportionality} + 5{,}463.8 \quad (7)$$

5. CONCLUSIONS

The present study investigates the mechanical performance of concretes reinforced with polymeric fibers, taking into account varying of the different levels (from 0% to 1,5% of V_f). The ensuing conclusions are derived from the results presented herein:

- the modulus of elasticity was found to be negatively impacted by the incorporation of fibers within concrete specimens. The compressive strength exhibited a greater susceptibility to alterations in fiber content compared to the specific type of concrete utilized.

- the optimal content of polypropylene macro fiber A, as determined by a comprehensive evaluation of the experimental results, was determined to be 1% (concrete C1.0A).
- the utilization of distinct fiber types (A, B, and C) with equivalent Vf exhibited minimal influence on the modulus of elasticity and residual flexural tensile strengths. The C1.0B concrete demonstrated superior performance in compressive strength, while the C1.0A concrete exhibited superior performance in the tensile strength test, particularly with regard to the limit of proportionality.
- concretes with fibers A and C exhibited a tendency towards decreased electrical resistivity, particularly surface electrical resistivity (up to a 19% reduction), while ultrasonic pulse velocity remained relatively constant. Conversely, the 1.0B concrete exhibited minimal variation in surface electrical resistivity and exhibited a modest increase in ultrasonic pulse velocity.
- the present study demonstrated a marked improvement in residual flexural tensile strengths with increasing fiber content, indicating that the FRC exhibited greater ductility.
- The FRC approach was found to be advantageous, particularly in concretes subjected to flexural tensile strength demands, as it resulted in an enhancement in flexural performance.
- In light of the minimal alterations observed in the other properties, a heightened focus on durability aspects is imperative. The performance of the three types of fibers studied (A, B, and C) was found to be "equivalent", with no significant differences observed between them. This finding serves to confirm the satisfactory performance of the fibers in relation to the concrete properties that were examined.

6. ACKNOWLEDGEMENTS

The authors thank Concrecon for providing the analyzed concrete and performing the compressive strength test; and LABITECC, the laboratory used for conducting the other tests.

7. BIBLIOGRAPHY

[1] MAZROA, A.A., ALOTAIBI, F.A., RAMAMURTHY, C., *et al.*, "Predictive modeling of cementitious green hybrid concrete strength for low-volume roads using RSM", *Matéria*, v. 30, pp. e20240603, 2025. doi: https://doi.org/10.1590/1517-7076-rmat-2024-0603.

[2] TIZA, M.T., "Sustainability in the civil engineering and construction industry: a review", *Journal of Sustainable Construction Materials and Technologies*, v. 7, n. 1, pp. 30–39, 2022. doi: https://doi.org/10.14744/jscmt.2022.11.

[3] CASCUDO, O., TEODORO, R., DE OLIVEIRA, A.M., *et al.*, "Effect of different metakaolins on chloride-related durability of concrete", *ACI Materials Journal*, v. 118, n. 3, pp. 3–14, 2021.

[4] BENTUR, A., MINDESS, S. *Fibre reinforced cementitious composites*, 2 ed., London, Elsevier Applied Science, 2007.

[5] MURUGAN, A., KALIAPPAN, S.P., SELVARAJAN, A.K., "Mechanical and durability investigation of fiber effect in finer concrete with various admixtures", *Matéria*, v. 30, pp. e20250219, 2025. doi: https://doi.org/10.1590/1517-7076-rmat-2025-0219.

[6] NACHIMUTHU, B., VASANTHARAJ, K., SOUNDARARAJAN, E.K., *et al.*, "Strength prediction of hybrid fiber reinforced self-compacting concrete using optimal recurrent neural network", *Matéria*, v. 30, pp. e20250150, 2025. doi: https://doi.org/10.1590/1517-7076-rmat-2025-0150.

[7] LONG, Z., LONG, G., ZHANG, Y., *et al.*, "Mechanical properties and damage analysis of polymer fiber reinforced concrete in low vacuum environments based on acoustic emission technology", *Journal of Radiological Science and Technology*, v. 1, n. 1, pp. 68–84, 2025. doi: https://doi.org/10.1016/j.jrst.2025.07.002.

[8] JUSTIN, S., THUSHANTHAN, K., THARMARAJAH, G., "Durability and mechanical performance of glass and natural fiber-reinforced concrete in acidic environments", *Construction & Building Materials*, v. 465, pp. 140262, 2025. doi: https://doi.org/10.1016/j.conbuildmat.2025.140262.

[9] FARHANGI, V., MORADI, M.J., DANESHVAR, K., *et al.*, "Application of artificial intelligence in predicting the residual mechanical properties of fiber reinforced concrete (FRC) after high temperatures", *Construction & Building Materials*, v. 411, pp. 134609, 2024. doi: https://doi.org/10.1016/j.conbuildmat.2023.134609.

[10] LU, S., LIU, J., TIAN, Z., *et al.*, "Deterioration mechanisms and strength prediction of hybrid fiber-reinforced concrete under coupled sulfate attack and dry-wet cycles", *Construction & Building Materials*, v. 493, pp. 143243, 2025. doi: https://doi.org/10.1016/j.conbuildmat.2025.143243.

[11] OLIVEIRA, A.M., SILVA, F.D.A., FAIRBAIRN, E.D.M.R., *et al.*, "Coupled temperature and moisture effects on the tensile behavior of strain hardening cementitious composites (SHCC) reinforced with PVA fibers", *Materials and Structures*, v. 51, n. 3, pp. 65, 2018. doi: https://doi.org/10.1617/s11527-018-1192-1.

[12] BALAGOPAL, V., PANICKER, A.S., ARATHY, M.S., *et al.*, "Influence of fibers on the mechanical properties of cementitious composites-a review", *Materials Today: Proceedings*, v. 65, pp. 1846–1850, 2022. doi: https://doi.org/10.1016/j.matpr.2022.05.023.

[13] MEHTA, P.K., MONTEIRO, P.J.M., *Concreto: estrutura, propriedades e materiais*, 2 ed., São Paulo, PINI, 2014.

[14] NEVILLE, A.M., *Propriedades do concreto*, São Paulo, PINI, 1997.

[15] AMERICAN CONCRETE INSTITUTE, *ACI Committee 544, 4R-18: Guide to Design with Fiber-Reinforced Concrete*, Indianápolis, ACI, 2018.

[16] BAŞSÜRÜCÜ, M., FENERLI, C., KINA, C., *et al.*, "Effect of fiber type, shape and volume fraction on mechanical and flexural properties of concrete", *Journal of Sustainable Construction Materials and Technologies*, v. 7, n. 3, pp. 158–171, 2022. doi: https://doi.org/10.47481/jscmt.1137088.

[17] CHAFEI, S., FREITAS DUTRA, L., JAMALI, A., "Enhancing mechanical behavior of cement composites through citric acid treatment of flax fibers", *Journal of Materials in Civil Engineering*, v. 36, n. 1, Jan. 2024. doi: https://doi.org/10.1061/JMCEE7.MTENG-15863.

[18] HOY, M., RO, B., HORPIBULSUK, S., *et al.*, "Flexural fatigue performance of hemp fiber–reinforced concrete using recycled concrete aggregates as a sustainable rigid pavement", *Journal of Materials in Civil Engineering*, v. 36, n. 11, Nov. 2024. doi: https://doi.org/10.1061/JMCEE7.MTENG-18367.

[19] FU, J., ZHOU, A., WU, Y., *et al.*, "Study on the stressing state features of basalt fibre concrete lining structure under sulphate erosion", *Construction & Building Materials*, v. 443, pp. 137723, Sept. 2024. doi: https://doi.org/10.1016/j.conbuildmat.2024.137723.

[20] SANKAR, B., ANITHA, D., ARUNKUMAR, K., *et al.*, "A study on the mechanical performance, shrinkage and morphology of high-performance fiber reinforced concrete with varying SCMs and geometry of steel fibers", *Case Studies in Construction Materials*, v. 21, pp. e03642, Dec. 2024. doi: https://doi.org/10.1016/j.cscm.2024.e03642.

[21] CARRILLO, J., SALCEDO, E., ROJAS, F., "Evaluating direct shear performance of steel fiber–reinforced concrete", *Journal of Materials in Civil Engineering*, v. 36, n. 2, Feb. 2024. doi: https://doi.org/10.1061/JMCEE7.MTENG-16532.

[22] VARMA, D.A., SARKER, P.K., MADHAVAN, M.K., *et al.*, "Performance comparison of Fiber Reinforced Polymer (FRP) systems and Textile Reinforced Mortar (TRM) for concrete confinement at elevated temperature", *Composites Part C: Open Access*, v. 17, pp. 100628, 2025. doi: https://doi.org/10.1016/j.jcomc.2025.100628.

[23] FENG, Y., LI, Z., FENG, J., *et al.*, "Multiscale analysis of EPS concrete strengthened by synergistic reinforcement of styrene–butadiene latex and PVA fibers: experiments and molecular dynamics simulations", *Journal of Materials in Civil Engineering*, v. 36, n. 11, Nov. 2024. doi: https://doi.org/10.1061/JMCEE7.MTENG-18211.

[24] ZOU, C., ZHENG, S., CHEN, Z., *et al.*, "Effects of aggregate preheating and polymer fibers on the mechanical, thermal and radiation shielding properties of barite concrete", *Construction & Building Materials*, v. 442, pp. 137533, Sept. 2024. doi: https://doi.org/10.1016/j.conbuildmat.2024.137533.

[25] YANG, W., HUANG, Y., LI, C., *et al.*, "Damage prediction and long-term cost performance analysis of glass fiber recycled concrete under freeze-thaw cycles", *Case Studies in Construction Materials*, v. 21, pp. e03795, 2024. doi: https://doi.org/10.1016/j.cscm.2024.e03795.

[26] BALAJI, G.R., SURIYA PRAKASH, S., "Effect of discrete fiber addition on the serviceability performance of glass fiber reinforced polymer concrete beams under flexure", *Structures*, v. 76, pp. 108901, 2025. doi: https://doi.org/10.1016/j.istruc.2025.108901.

[27] AHMAD, J., ZHOU, Z., "Mechanical properties of natural as well as synthetic fiber reinforced concrete: a review", *Construction & Building Materials*, v. 333, pp. 127353, May. 2022. doi: https://doi.org/10.1016/j.conbuildmat.2022.127353.

[28] SWOLFS, Y., ZHANG, Q., BAETS, J., *et al.*, "The influence of process parameters on the properties of hot compacted self-reinforced polypropylene composites", *Composites. Part A, Applied Science and Manufacturing*, v. 65, pp. 38–46, Oct. 2014. doi: https://doi.org/10.1016/j.compositesa.2014.05.022.

[29] EUROPEAN COMMITTEE FOR STANDARDIZATION, *EN 14889-2: Fibres for Concrete - Part 2: Polymer Fibres - Definitions, Specifications and Conformity*, Brussels, CEN, 2008.

[30] ASSOCIAÇÃO BRASILEIRA DE NORMAS TÉCNICAS, *ABNT: NBR 15530, fibras de aço para concreto — Requisitos e métodos de ensaio - Concrete steel fibers — Requirements and test methods*, Rio de Janeiro, ABNT, 2019.

[31] AMERICAN SOCIETY FOR TESTING AND MATERIALS, *ASTM A820-01 Standard Specification for Steel Fibers for Fiber-Reinforced Concrete*, West Conshohocken, ASTM, 2021.

[32] ASSOCIAÇÃO BRASILEIRA DE NORMAS TÉCNICAS, *ABNT: NBR7481, Tela de aço soldada nervurada para armadura de concreto – Requisitos*, Rio de Janeiro, ABNT, 2022.

[33] AMERICAN SOCIETY FOR TESTING AND MATERIAL, *STM F2919/F2919M-12, Standard Specification for Welded Wire Mesh Fence Fabric (Metallic-Coated or Polymer Coated) with Variable Mesh Patterns or Meshes Greater than 6 in.2 [3871 mm2] in Panels*, West Conshohocken, ASTM, 2018.

[34] VIAPOL, *Ficha Técnica de Produto, TUF STRAND SF*, Caçapava, Viapol, 2013.

[35] OZTURK, O., OZYURT, N., "Sustainability and cost-effectiveness of steel and polypropylene fiber reinforced concrete pavement mixtures", *Journal of Cleaner Production*, v. 363, pp. 132582, Aug. 2022. doi: https://doi.org/10.1016/j.jclepro.2022.132582.

[36] ASSOCIAÇÃO BRASILEIRA DE NORMAS TÉCNICAS, *ABNT PR 1011: Projeto de pavimentos urbanos em concreto / Associação Brasileira de Normas Técnicas*, Rio de Janeiro, ABNT, 2021.

[37] AMERICAN CONCRETE INSTITUTE, *ACI PRC-325.12-02: Guide for Design of Jointed Concrete Pavements for Streets and Local Roads*, Indianapolis, ACI, 2019.

[38] AMERICAN CONCRETE INSTITUTE, *ACI PRC-330.2-17: Guide for the Design and Construction of Concrete Site Paving for Industrial and Trucking Facilities*, Indianapolis, ACI, 2020.

[39] PENA, P.V.C., FERREIRA, R.A.R., SANTOS, A.C., *et al.*, "Analysis of the compressive creep strain of the concretes with steel fibers: a holistic view in micro and macro scale", *Journal of Building Engineering*, v. 71, pp. 106436, 2023. doi: https://doi.org/10.1016/j.jobe.2023.106436.

[40] PALANISAMY, E., RAMASAMY, M., "Dependency of sisal and banana fiber on mechanical and durability properties of polypropylene hybrid fiber reinforced concrete", *Journal of Natural Fibers*, v. 19, n. 8, pp. 3147–3157, 2022. doi: https://doi.org/10.1080/15440478.2020.1840477.

[41] ISLAM, S.U., WASEEM, S.A., "An experimental study on mechanical and fracture characteristics of hybrid fibre reinforced concrete", *Structures*, v. 68, pp. 107053, 2024. doi: https://doi.org/10.1016/j.istruc.2024.107053.

[42] CASTOLDI, R.S., SOUZA, L.M.S., SILVA, F.A., "Comparative study on the mechanical behavior and durability of polypropylene and sisal fiber reinforced concretes", *Construction & Building Materials*, v. 211, pp. 617–628, 2019. doi: https://doi.org/10.1016/j.conbuildmat.2019.03.282.

[43] ZHANG, Y., ASLANI, F., "Mechanical and ultrasonic pulse velocity performance of 3D printed rubberised cementitious composites reinforced with PVA fibres", *Journal of Building Engineering*, v. 112, pp. 113886, 2025. doi: https://doi.org/10.1016/j.jobe.2025.113886.

[44] TORRIJOS, M.C., BARRAGAN, B.E., ZERBINO, R.L., "Physical-mechanical properties, and mesostructure of plain and fibre reinforced self-compacting concrete", *Construction & Building Materials*, v. 22, n. 8, pp. 1780–1788, 2008. doi: https://doi.org/10.1016/j.conbuildmat.2007.05.008.

[45] NEMATZADEH, M., TAYEBI, M., SAMADVAND, H., "Prediction of ultrasonic pulse velocity in steel fiber-reinforced concrete containing nylon granule and natural zeolite after exposure to elevated temperatures", *Construction & Building Materials*, v. 273, pp. 121958, 2021. doi: https://doi.org/10.1016/j.conbuildmat.2020.121958.

[46] SILVA, L.A., ASSIS LEONEL, A.C., OLIVEIRA, A.M.D.O., "Efeito de cloretos e da umidade interna de concretos na resistividade elétrica superficial e volumétrica: influência na especificação de concretos duráveis", *Paranoá*, v. 18, pp. e53272, 2025. doi: https://doi.org/10.18830/1679-09442025v18e53272.

[47] MALHOTRA, V.M., CARINO, N.J., *Handbook on nondestructive testing of concrete*, West Conshohocken, ASTM International, pp. 2–13, 2004.

[48] CÁNOVAS, M.F., *Patologia e terapia do concreto armado*, São Paulo, Ed. Pini, 1998.

[49] ACEBES, M., MOLERO, M., SEGURA, I., *et al.*, "Study of the influence of microstructural parameters on the ultrasonic velocity in steel–fiber-reinforced cementitious materials", *Construction & Building Materials*, v. 25, n. 7, pp. 3066–3072, 2011. doi: https://doi.org/10.1016/j.conbuildmat.2010.12.062.

[50] ALHARTHAI, M., ALI, T., QURESHI, M.Z., *et al.*, "The enhancement of engineering characteristics in recycled aggregates concrete combined effect of fly ash, silica fume and PP fiber", *Alexandria Engineering Journal*, v. 95, pp. 363–375, May. 2024. doi: https://doi.org/10.1016/j.aej.2024.03.084.

[51] CASTILLO, D., HEDJAZI, S., "Early-age compressive strength and dynamic modulus of FRC based on ultrasonic pulse velocity", *Materiales de Construcción*, v. 71, n. 343, pp. e257, 2021. doi: https://doi.org/10.3989/mc.2021.14720.

[52] YAZICI, Ş., İNAN, G., TABAK, V., "Effect of aspect ratio and volume fraction of steel fiber on the mechanical properties of SFRC", *Construction & Building Materials*, v. 21, n. 6, pp. 1250–1253, 2007. doi: https://doi.org/10.1016/j.conbuildmat.2006.05.025.

[53] LEONEL, A.C.A., OLIVEIRA, A.M., CASCUDO, O., "Interação da resistividade elétrica com esclerometria e velocidade de propagação de ondas ultrassônicas", *Paranoá*, v. 17, pp. e49960, 2024. doi: https://doi.org/10.18830/1679-09442024v17e49960.

[54] DE MEDEIROS, M.H.F., LOPES, R.C., REAL, L.V., *et al.*, "Efeito do tipo de cimento e de materiais cimentícios suplementares na resistividade elétrica superficial do concreto", *Ambiente Construído*, v. 25, pp. e140952, 2025. doi: https://doi.org/10.1590/s1678-86212025000100874.

[55] ROBLES, K.P., GUCUNSKI, N., KEE, S.-H., "Evaluation of steel corrosion-induced concrete damage using electrical resistivity measurements", *Construction & Building Materials*, v. 411, pp. 134512, 2024. doi: https://doi.org/10.1016/j.conbuildmat.2023.134512.

[56] JI, H., TIAN, Y., FU, C., *et al.*, "Transfer learning enables prediction of steel corrosion in concrete under natural environments", *Cement and Concrete Composites*, v. 148, pp. 105488, 2024. doi: https://doi.org/10.1016/j.cemconcomp.2024.105488.

[57] BANG, J.B., YIM, H.J., "Segregation evaluation of concrete pavements under excessive vibration using electrical resistivity measurement", *Case Studies in Construction Materials*, v. 19, pp. e02300, 2023. doi: https://doi.org/10.1016/j.cscm.2023.e02300.

[58] ESAKER, M., HAMZA, O., ELLIOTT, D., "Monitoring the bio-self-healing performance of cement mortar incubated within soil and water using electrical resistivity", *Construction & Building Materials*, v. 393, pp. 132109, 2023. doi: https://doi.org/10.1016/j.conbuildmat.2023.132109.

[59] LUJÁN, V.F., MALDONADO-GARCÍA, M.A.M, QUERO, V.G.J., *et al.*, "Reliability of electrical resistivity on the long-term monitoring of concrete", *Construction & Building Materials*, v. 18, pp. 101154, 2023. doi: https://doi.org/10.1016/j.rineng.2023.101154.

[60] SENGUL, O., GJØRV, O.E., "Effect of embedded steel on electrical resistivity measurements on concrete structures", *ACI Materials Journal*, v. 106, n. 1, pp. 11, 2009. doi: https://doi.org/10.14359/56311.

[61] OLIVEIRA, A.M., CASCUDO, O., "Effect of mineral additions incorporated in concrete on thermodynamic and kinetic parameters of chloride-induced reinforcement corrosion", *Construction & Building Materials*, v. 192, pp. 467–477, 2018. doi: https://doi.org/10.1016/j.conbuildmat.2018.10.100.

[62] YIM, H.J., BAE, Y.H., KIM, J.H., "Method for evaluating segregation in self-consolidating concrete using electrical resistivity measurements", *Construction & Building Materials*, v. 232, pp. 117283, 2020. doi: https://doi.org/10.1016/j.conbuildmat.2019.117283.

[63] CHEYTANI, M., CHAN, S.L.I., "The applicability of the Wenner method for resistivity measurement of concrete in atmospheric conditions", *Case Studies in Construction Material*, v. 15, pp. e00663, 2021. doi: https://doi.org/10.1016/j.cscm.2021.e00663.

[64] ARAÚJO, E.C., MACIOSKI, G., DE MEDEIROS, M.H.F., "Concrete surface electrical resistivity: effects of sample size, geometry, probe spacing and SCMs", *Construction & Building Materials*, v. 324, pp. 126659, 2022. doi: https://doi.org/10.1016/j.conbuildmat.2022.126659.

[65] MELARA, E.K., TRENTIN, P.O., PEREIRA, E., *et al.*, "Contribution to the service-life modeling of concrete exposed to sulfate attack by the inclusion of electrical resistivity data", *Construction & Building Materials*, v. 322, pp. 126490, 2022. doi: https://doi.org/10.1016/j.conbuildmat.2022.126490.

[66] LEONEL, A.C.A., OLIVEIRA, A.M., CASCUDO, O., "Interaction of electrical resistivity with rebound hammer and ultrasonic velocity test", *Paranoá*, v. 17, pp. 1–24, 2024.

[67] SATHIPARAN, N., JEYANANTHAN, P., SUBRAMANIAM, D.N., "Surface response regression and machine learning techniques to predict the characteristics of pervious concrete using non-destructive measurement: ultrasonic pulse velocity and electrical resistivity", *Measurement: Journal of the International Measurement Confederation*, v. 225, pp. 114006, 2024. doi: https://doi.org/10.1016/j.measurement.2023.114006.

[68] LATASTE, J.-F., VILLAIN, G., BALAYSSAC, J.-P., "Electrical methods", In: Balayssac, J.-P., Garnier, V. (eds), *Non-Destructive Testing and Evaluation of Civil Engineering Structures*, Amsterdam, Elsevier, pp. 139–172, 2018. doi: https://doi.org/10.1016/B978-1-78548-229-8.50004-2.

[69] CHEN, C.-T., CHANG, J.-J., YEIH, W., "The effects of specimen parameters on the resistivity of concrete", *Construction & Building Materials*, v. 71, pp. 35–43, Nov. 2014. doi: https://doi.org/10.1016/j.conbuildmat.2014.08.009.

[70] SPRAGG, R., VILLANI, C., SNYDER, K., *et al.*, "Factors that influence electrical resistivity measurements in cementitious systems", *Transportation Research Record: Journal of the Transportation Research Board*, v. 2342, n. 1, pp. 90–98, 2013. doi: https://doi.org/10.3141/2342-11.

[71] CASCUDO, O., *O controle da corrosão em armaduras de concreto: inspeção e técnicas eletroquímicas*, Goiânia, Editora UFG, 1997.

[72] MEDEIROS JUNIOR, R.D., MUNHOZ, G.D.S., MEDEIROS, M.D., "Correlations between water absorption, electrical resistivity and compressive strength of concrete with different contents of pozzolan", *Revista ALCONPAT*, v. 9, n. 2, pp. 152–166, 2019. doi: https://doi.org/10.21041/ra.v9i2.335.

[73] DINAKAR, P., BABU, K.G., SANTHANAM, M., "Corrosion behavior of blended cements in low and medium strength concretes", *Cement and Concrete Composites*, v. 29, n. 2, pp. 136–145, 2007. doi: https://doi.org/10.1016/j.cemconcomp.2006.10.005.

[74] LUBECK, A., GASTALDINI, A.L.G., BARIN, D.S., *et al.*, "Compressive strength and electrical properties of concrete with white Portland cement and blast -furnace slag", *Cement and Concrete Composites*, v. 34, n. 3, pp. 392–399, 2022. doi: https://doi.org/10.1016/j.cemconcomp.2011.11.017.

[75] ARAÚJO, C.C., MEIRA, G.R., "Correlation between concrete strength properties and surface electrical resistivity", *Revista IBRACON de Estruturas e Materiais*, v. 15, n. 1, pp. e15103, 2022. doi: https://doi.org/10.1590/s1983-41952022000100003.

[76] TANG, M., CHEN, X., LUO, Y., *et al.*, "Carbon fiber and PVA fiber reinforced concrete: Electrical resistivity and piezoresistive properties", *Materials Letters*, v. 376, pp. 137288, Dec. 2024. doi: https://doi.org/10.1016/j.matlet.2024.137288.

[77] DIAB, S.H., SOLIMAN, A.M., NOKKEN, M., "Performance-based design for fiber-reinforced concrete: potential balancing corrosion risk and strength", *Journal of Materials in Civil Engineering*, v. 32, n. 2, Feb. 2020. doi: https://doi.org/10.1061/(ASCE)MT.1943-5533.0003037.

[78] ASSOCIAÇÃO BRASILEIRA DE NORMAS TÉCNICAS, *NBR 16935: Projeto de estruturas de concreto reforçado com fibras — Procedimento*, Rio de Janeiro, ABNT, pp. 27, 2021.

[79] ASSOCIAÇÃO BRASILEIRA DE NORMAS TÉCNICAS, *NBR 16938: Concreto reforçado com fibras - Controle da qualidade*, Rio de Janeiro, ABNT, p. 12, 2021.

[80] ASSOCIAÇÃO BRASILEIRA DE NORMAS TÉCNICAS, *NBR 16940: Concreto reforçado com fibras - Determinação das resistências à tração na flexão (limite de proporcionalidade e resistências residuais) - Método de ensaio*, Rio de Janeiro, ABNT, p. 11, 2021.

[81] EUROPEAN STANDARD, *EN 14651, Test method for metallic fiber-reinforced concrete – Measuring the flexural tensile strength (limit of proportionality (LOP), residual)*, London, EN, pp. 1–15, 2007.

[82] ASSOCIAÇÃO BRASILEIRA DE NORMAS TÉCNICAS, *Prática Recomendada: ABNT PR 1011: Projeto de pavimentos urbanos em concreto*, Rio de Janeiro, ABNT, 2021.

[83] AMERICAN CONCRETE INSTITUTE, *ACI PRC-325.12-02: Guide for Design of Jointed Concrete Pavements for Streets and Local Roads*, Indianápolis, ACI, 2019.

[84] AMERICAN CONCRETE INSTITUTE, *ACI PRC-330.2-17: Guide for the Design and Construction of Concrete Site Paving for Industrial and Trucking Facilities (Reapproved 2020)*, Indianápolis, ACI, 2020.

[85] ASSOCIAÇÃO BRASILEIRA DE NORMAS TÉCNICAS, *NBR 16697: Cimento Portland — Requisitos (Portland cement — Requirements)*, Rio de Janeiro, ABNT, 2018.

[86] AMERICAN SOCIETY FOR TESTING MATERIAL, *ASTM C150/C150M-24, Standard Specification for Portland Cement*, West Conshohocken, ASTM, 2024.

[87] ASSOCIAÇÃO BRASILEIRA DE NORMAS TÉCNICAS, *ABNT NBR 7211, Agregados para concreto – Especificação* Rio de Janeiro, ABNT, 2005.

[88] AMERICAN SOCIETY FOR TESTING MATERIAL, *ASTM C33/C33M-18 - Standard Specification for Concrete Aggregates*, West Conshohocken, ASTM, 2023.

[89] ASSOCIAÇÃO BRASILEIRA DE NORMAS TÉCNICAS, *ABNT NBR 11768-1, Aditivos químicos para concreto de cimento Portland – Parte 1: Requisitos*, Rio de Janeiro, ABNT, 2019.

[90] AMERICAN SOCIETY FOR TESTING MATERIAL, *ASTM C494 for chemical admixtures*, West Conshohocken, ASTM, 2020.

[91] ASSOCIAÇÃO BRASILEIRA DE NORMAS TÉCNICAS, *ABNT NBR 15900-1, Água para amassamento do concreto – Parte 1: Requisito*, Rio de Janeiro, ABNT, 2009.

[92] AMERICAN SOCIETY FOR TESTING MATERIAL, *ASTM C1602/C1602M-22 Standard Specification for Mixing Water Used in the Production*, West Conshohocken, ASTM, 2022.

[93] ASSOCIAÇÃO BRASILEIRA DE NORMAS TÉCNICAS, *ABNT NBR 16942 Fibras poliméricas para concreto — Requisitos e métodos de ensaio - Polymers fibers for concrete — Requirements and test methods*, Rio de Janeiro, ABNT, 2021.

[94] AMERICAN SOCIETY FOR TESTING MATERIAL, *ASTM C1116/C1116M-10a (2015) - Standard Specification for Fiber-Reinforced Concrete*, West Conshohocken, ASTM, 2015.

[95] ASSOCIAÇÃO BRASILEIRA DE NORMAS TÉCNICAS, *NBR 16939: Concreto reforçado com fibras - Determinação das resistências à fissuração e residuais à tração por duplo puncionamento - Método de ensaio*, Rio de Janeiro, ABNT, p. 6, 2021.

[96] AMERICAN CONCRETE INSTITUTE, *ACI, 360 R-10, Guide to Design of Slabs-on-Ground*, Indianápolis, ACI, 2010.

[97] ASSOCIAÇÃO BRASILEIRA DE NORMAS TÉCNICAS, *NBR 14931 - Execução de estruturas de concreto armado, protendido e com fibras — Requisitos - Execution of reinforced, prestressed and fiber concrete structures — Procedure*, Rio de Janeiro, ABNT, 2023.

[98] ASSOCIAÇÃO BRASILEIRA DE NORMAS TÉCNICAS, *NBR 8953: Concreto para fins estruturais - Classificação pela massa específica, por grupos de resistência e consistência*, Rio de Janeiro, ABNT, 2015.

[99] ASSOCIAÇÃO BRASILEIRA DE NORMAS TÉCNICAS, *ABNT NBR16889, Concreto — Determinação da consistência pelo abatimento do tronco de cone*, Rio de Janeiro, ABNT, 2020.

[100] ASSOCIAÇÃO BRASILEIRA DE NORMAS TÉCNICAS, *NM67. Concreto - Determinação da consistência pelo abatimento do tronco de cone*, Rio de Janeiro, ABNT, 1996.

[101] AMERICAN SOCIETY FOR TESTING MATERIAL, *ASTM C143/C143M-12, Standard Test Method for Slump of Hydraulic-Cement Concrete*, West Conshohocken, ASTM, 2015.

[102] ASSOCIAÇÃO BRASILEIRA DE NORMAS TÉCNICAS, *NBR5738: Concreto - Procedimento para Moldagem e Cura de Corpos de Prova*, Rio de Janeiro, ABNT, 2015.

[103] ASSOCIAÇÃO BRASILEIRA DE NORMAS TÉCNICAS, *NBR5739: Concreto - Ensaio de Compressão de Corpos de Prova Cilíndricos*, Rio de Janeiro, ABNT, 2018.

[104] AMERICAN SOCIETY FOR TESTING MATERIAL, *ASTM C39/C39M: Standard Test Method for Compressive Strength of Cylindrical Concrete Specimens*, West Conshohocken, ASTM, 2023.

[105] EUROPEAN STANDARD, *EN 206 Concrete – Specification, Performance, Production and Conformity*, London, EN, 2013.

[106] ASSOCIAÇÃO BRASILEIRA DE NORMAS TÉCNICAS, *ABNT NBR 8522-1: 2021*, Rio de Janeiro, ABNT, 2021.

[107] AMERICAN SOCIETY FOR TESTING MATERIAL, *ASTM C469/C469M-22 Standard Test Method for Static Modulus of Elasticity and Poisson's Ratio of Concrete in Compression*, West Conshohocken, ASTM, p. 6, 2022.

[108] AMERICAN SOCIETY FOR TESTING MATERIAL, *ASTM C1609-12, Standard Test Method for Flexural Performance of Fiber-Reinforced Concrete (Using Beam with Third-Point Loading)*, West Conshohocken, ASTM, 2019.

[109] MATERIALS AND STRUCTURES, "Determination of the fracture energy of mortar and concrete by means of three-point bend tests on notched beames", *Materials and Structures*, v. 18, n. 106, pp. 285–290, 1985.

[110] AMERICAN SOCIETY FOR TESTING MATERIAL, *ASTM G57-22: Standard Test Method for Measurement of Soil Resistivity Using the Wenner Four-Electrode Method*, West Conshohocken, ASTM, 2020.

[111] AMERICAN SOCIETY FOR TESTING MATERIAL, *ASTM C1876-24: Standard Test Method for Bulk Electrical Resistivity or Bulk Conductivity of Concrete*, West Conshohocken, ASTM, 2024.

[112] BRITISH STANDARDS, *BS 1881: Part 203, 1986 -. ACI 228.2R. Nondestructive Test Methods for Evaluation of Concrete in Structures*, Farmington Hills, BS, 2013.

[113] AMERICAN SOCIETY FOR TESTING MATERIAL, *ASTM C597-22: Standard Test Method for Pulse Velocity Through Concrete*, West Conshohocken, ASTM, 2023.

[114] EUROPEAN STANDARD, *EN 12504-4.Testing concrete in structures. Part 4: Determination of ultrasonic pulse velocity*, London, EN, 2004.

[115] PROCEQ SA, *Instruções de operação Teste de durabilidade do concreto*, Schwerzenbach, Proceq, 2017.

[116] EUROPEAN STANDARD, *UNE 83988-2: UNE 83988-2. Concrete durability. Test methods. Determination of the electrical resistivity. Part 2: Four points or Wenner method*, London, EN, 2014.

[117] WATTS, M.J., AMIN, A., BERNARD, E.S., *et al.*, "Early age bond stress-slip behaviour of macro-synthetic fibre reinforced concrete", *Construction & Building Materials*, v. 301, pp. 124097, Sept. 2021. doi: https://doi.org/10.1016/j.conbuildmat.2021.124097.

[118] LATIFI, M.R., BIRICIK, Ö., MARDANI, A., "Mechanical and durability performance of macro polypropylene fibrous concrete", *Iranian Polymer Journal*, v. 32, n. 9, pp. 1149–1164, Sept. 2023. doi: https://doi.org/10.1007/s13726-023-01193-6.

[119] ABOUSNINA, R., PREMASIRI, S., ANISE, V., *et al.*, "Mechanical properties of macro polypropylene fibre-reinforced concrete", *Polymers*, v. 13, n. 23, pp. 4112, Nov. 2021. doi: https://doi.org/10.3390/polym13234112. PubMed PMID: 34883614.

[120] LATIFI, M.R., BIRICIK, Ö., MARDANI AGHABAGLOU, A., "Effect of the addition of polypropylene fiber on concrete properties", *Journal of Adhesion Science and Technology*, v. 36, n. 4, pp. 345–369, Feb. 2022. doi: https://doi.org/10.1080/01694243.2021.1922221.

[121] BAŞSÜRÜCÜ, M., FENERLI, C., KINA, C., *et al.*, "Effect of fiber type, shape and volume fraction on mechanical and flexural properties of concrete", *Journal of Sustainable Construction Materials and Technologies*, v. 7, n. 3, pp. 158–171, 2022. doi: https://doi.org/10.47481/jscmt.1137088.

[122] EWA, D., UKPATA, J., ETIKA, A., *et al.*, "A comparative evaluation of the mechanical properties of PET and polystyrene modified asphaltic concrete containing rice husk ash filler", *Journal of Sustainable Construction Materials and Technologies*, v. 9, n. 1, pp. 84–92, 2024. doi: https://doi.org/10.47481/jscmt.1166150.

[123] DEHGHANPOUR, H., DOĞAN, F., SUBAŞI, S., *et al.*, "Effects of single-walled carbon nanotubes and steel fiber on recycled ferrochrome filled electrical conductive mortars", *Journal of Sustainable Construction Materials and Technologies*, v. 7, n. 4, pp. 250–265, 2022. doi: https://doi.org/10.47481/jscmt.1163963.

[124] SIVAKUMAR, A., SANTHANAM, M., "A quantitative study on the plastic shrinkage cracking in high strength hybrid fibre reinforced concrete", *Cement and Concrete Composites*, v. 29, n. 7, pp. 575–581, Aug. 2007. doi: https://doi.org/10.1016/j.cemconcomp.2007.03.005.

[125] FIB INTERNATIONAL FEDERATION FOR STRUCTURAL CONCRETE, *fib Model code for concrete structures*, Lausanne, FIB, 2010.

[126] MONTEIRO, V.M.A., LIMA, L.R., SILVA, F.A., "On the mechanical behavior of polypropylene, steel and hybrid fiber reinforced self-consolidating concrete", *Construction & Building Materials*, v. 188, pp. 280–291, Nov. 2018. doi: https://doi.org/10.1016/j.conbuildmat.2018.08.103.

[127] AMGAD, J., HAMMAD, N., EL-NEMR, A.M., "Correlation of non-destructive with mechanical tests for self-compacting concrete (SCC)", In: Shehata, H.F. (eds), *Sustainable Civil Infrastructures*, Berlin, Springer International Publishing, pp. 238–246, 2021.

[128] DE OLIVEIRA, A.M., CASCUDO, O., "Effect of mineral additions incorporated in concrete on thermodynamic and kinetic parameters of chloride-induced reinforcement corrosion", *Construction & Building Materials*, v. 192, pp. 467–477, 2018. doi: https://doi.org/10.1016/j.conbuildmat.2018.10.100.

[129] OLIVEIRA, A.M., SILVA, F.D.A., FAIRBAIRN, E.D.M.R., *et al.*, "Coupled temperature and moisture effects on the tensile behavior of strain hardening cementitious composites (SHCC) reinforced with PVA fibers", *Materials and Structures*, v. 51, n. 3, pp. 65, 2018. doi: https://doi.org/10.1617/s11527-018-1192-1.

[130] SADEGHI NIK, A., LOTFI OMRAN, O., "Estimation of compressive strength of self-compacted concrete with fibers consisting nano-SiO2 using ultrasonic pulse velocity", *Construction & Building Materials*, v. 44, pp. 654–662, 2013. doi: https://doi.org/10.1016/j.conbuildmat.2013.03.082.

[131] RAHMANI, E., DEHESTANI, M., BEYGI, M.H.A., *et al.*, "On the mechanical properties of concrete containing waste PET particles", *Construction & Building Materials*, v. 47, pp. 1302–1308, 2013. doi: https://doi.org/10.1016/j.conbuildmat.2013.06.041.

[132] BARIŞ, K.E., TANAÇAN, L., "Research on the long-term strength development of Datça Pozzolan-based geopolymer", *Journal of Sustainable Construction Materials and Technologies*, v. 9, n. 1, pp. 11–24, 2024. doi: https://doi.org/10.47481/jscmt.1406171.

[133] GODINHO, J.P., DE SOUZA, T.F., MEDEIROS, M.H.F., "Factors influencing ultrasonic pulse velocity in concrete", *Revista IBRACON de Estruturas e Materiais*, v. 13, n. 02, pp. 222–247, 2020. doi: https://doi.org/10.1590/s1983-41952020000200004.

[134] ZHANG, Y., ASLANI, F., "Mechanical and ultrasonic pulse velocity performance of 3D printed rubberised cementitious composites reinforced with PVA fibres", *Journal of Building Engineering*, v. 112, pp. 113886, 2025. doi: https://doi.org/10.1016/j.jobe.2025.113886.

[135] DEL SAVIO, A.A., LA TORRE ESQUIVEL, D., CARRILLO, J., *et al.*, "Determination of polypropylene fiber-reinforced concrete compressive strength and elasticity modulus via ultrasonic pulse tests", *Applied Sciences*, v. 12, n. 20, pp. 10375, 2022. doi: https://doi.org/10.3390/app122010375.

[136] KOZŁOWSKI, M., KADELA, M., KUKIEŁKA, A., "Fracture energy of foamed concrete based on three-point bending test on notched beams", *Procedia Engineering*, v. 108, pp. 349–354, 2015. doi: https://doi.org/10.1016/j.proeng.2015.06.157.

[137] ZHOU, W., MO, J., ZENG, L., *et al.*, "Fracture behavior of polypropylene fiber reinforced concrete modified by rubber powder exposed to elevated temperatures", *Construction & Building Materials*, v. 346, pp. 128439, 2022. doi: https://doi.org/10.1016/j.conbuildmat.2022.128439.